Early Miocene carbonate ramp development in a warm ocean, North West Shelf, Australia

ROSINE RIERA *, † iD , JULIEN BOURGET *, TONY ALLAN ‡, ECKART HÅKANSSON * and MOYRA E. J. WILSON *

School of Earth Sciences, Centre for Energy Geoscience, The University of Western Australia, Perth, WA, 6009, Australia
†*Norwegian Geotechnical Institute, Level 7, 40 St Georges Terrace, Perth, WA, 6000, Australia*
(E-mail: rosine.riera@ngi.no)
‡*Environmental Geochemistry International, 81A College Street, Balmain, NSW, 2041, Australia*

ABSTRACT

Although carbonate ramps are widely described from the geological record, there is still a debate on the relative influence of water temperature, trophic conditions and type of carbonate factories on their development. The *ca* 2400 km long Australian North West Shelf is among the largest Cenozoic carbonate provinces worldwide, and records a transition from an early Miocene ramp to a middle Miocene rimmed platform. This change is observable on publicly available seismic data, giving the opportunity to investigate environmental influences on platform evolution. This study combines macroscopic and petrographic descriptions of early Miocene strata cropping out in the Cape Range Anticline (North West Cape, southern end of the North West Shelf) and of time-equivalent well cuttings from the adjacent, offshore Exmouth Sub-basin. Particular emphasis is placed on the identification of larger benthic foraminifera at a broad generic level, because differing taxa have a limited range of habitable conditions that serve as environmental proxies. The results show that early Miocene strata are dominantly composed of larger benthic foraminifera with minor coralline algae in the proximal platform, grading to micropackstones in the more distal platform. A ramp margin is inferred from the lithological data on the basis of the lack of framework builders and the presence of open oceanic indicators. Facies shallow upward through individual outcrops, with a proximal to distal trend towards the north-west. These trends along outcrops are consistent with the seismic interpretations. Identification of taxa with warm, oligotrophic water affinity suggests that the ramp was formed in an oligotrophic and warm ocean, despite the absence of coral reefs. Changes of carbonate facies with depth do not seem to be associated with changes in ramp morphology, and the latter may have been controlled by physical oceanic parameters, such as offshore currents and waves.

Keywords Australia, Burdigalian, carbonate platform, distally steepened ramp, facies, larger benthic foraminifera, Leeuwin current, Miocene Climatic Optimum.

INTRODUCTION

Establishing the role of environmental factors on the formation of carbonate ramps versus rimmed carbonate platforms has been a subject of debate for the last 30 years. Oligo–Miocene examples have been particularly well-investigated with studies addressing this question in the Mediterranean Sea region (Pomar, 2001a; Mateu-Vicens *et al.*, 2008; Pomar & Kendall, 2008; Westphal *et al.*, 2010; Brandano *et al.*, 2017; Pomar *et al.*, 2017), south-east Asia (Wilson & Vecsei, 2005; Teillet *et al.*, 2020), Australia (James & Borch, 1991; Feary & James, 1995; Isern *et al.*, 1996; Betzler, 1997; Conesa *et al.*, 2005; O'Connell *et al.*, 2012; Rosleff-Soerensen *et al.*, 2012, 2016) and the western Pacific Ocean (Maurizot *et al.*, 2016). Combining interpretation of outcrops with regional subsurface seismic data is an important approach for identifying the dominant controls on ramp and rimmed platform morphology, and how facies are distributed across these platform profiles (Bosence, 2005). The modern North West Shelf (NWS; Purcell & Purcell, 1988) of Australia is an ocean-facing high-energy carbonate-dominated ramp (fair-weather wave base at *ca* 50 m, storm-wave base at *ca* 115 m and swell-wave base at *ca* 300 m; James *et al.*, 2004), that extends over *ca* 2400 km along the semi-arid north-western coast of Australia (Groeneveld *et al.*, 2017). Although this ramp is located on a western continental margin, strong coastal upwellings are absent and marine waters along the NWS are tropical. This unique setting is partly due to the presence of the warm (28 to 30°C) south-flowing Leeuwin Current (Hatcher, 1991; Smith, 1992; James *et al.*, 2004; Collins *et al.*, 2014). This *ca* 100 km wide current strongly influences water movement in the upper 300 m of the water column, and reaches a maximum speed of 0.25 cm s^{-1} at the shelf break (James *et al.*, 2004). Modern sediments along the NWS are aragonite-poor, with fine sediments predominantly composed of calcitic bioclasts and minor quartz grains (Hallenberger *et al.*, 2019). In contrast, during the last glacial maximum, which was an arid period (Deckker *et al.*, 2014; Gallagher *et al.*, 2014; Stuut *et al.*, 2014; Kuhnt *et al.*, 2015) inorganic aragonite precipitation was widespread (Dix *et al.*, 2005; Hallenberger *et al.*, 2019). High aragonite precipitation rates may have been possible through increased aridity and absence of river runoff (James *et al.*, 2004; Hallenberger *et al.*, 2019) and/or by the changes in inherited platform geometry, with lowered sea-level transforming the extensive and open NWS into a narrow and protected platform (Dix *et al.*, 2005).

During the early Miocene, sedimentation along the NWS was also occurring along a ramp profile (Fig. 1). This ramp evolved into a rimmed platf (*sensu* Bosence, 2005) during the middle Miocene (Jones, 1973; Bradshaw *et al.*, 1988; Romine *et al.*, 1997; Young *et al.*, 2001; Collins, 2002; Gorter *et al.*, 2002; Cathro *et al.*, 2003; Power, 2008; Ryan *et al.*, 2009; Liu *et al.*, 2011; Rosleff-Soerensen *et al.*, 2012, 2016; Saqab & Bourget, 2016; Belde *et al.*, 2017; Rankey, 2017; Tuyl *et al.*, 2018a,b; Anell & Wallace, 2019; Tuyl *et al.*, 2019; McCaffrey *et al.*, 2020). Whilst this transition is one of the largest Cenozoic ramp to rimmed platform transitions recognized [for example, compilation of major Phanerozoic reef trends by Kiessling (2001)], controlling factors remain the subject of debate.

Seismic-based and offshore-well-based studies interpret the ramp as a prograding system dominantly composed of fine detrital carbonate sediments, with occasional clay and/or bioclasts, such as bryozoans in the older, deeper facies, and echinoids and larger foraminifera in the younger, shallower facies (Apthorpe, 1988; Young, 2001; Moss *et al.*, 2004). Most seismic-based studies classify the ramp as a heterozoan system (cf. James, 1997; Michel *et al.*, 2018) and commonly interpret the presence of the ramp morphology as indicative of cool to sub-tropical climatic conditions (e.g. Cathro *et al.*, 2003; Rosleff-Soerensen *et al.*, 2012; Belde *et al.*, 2017; Rankey, 2017; Rinke-Hardekopf *et al.*, 2018; Anell & Wallace, 2019; McCaffrey *et al.*, 2020). In the absence of core, offshore lithological observations are, however, limited to discontinuous well cuttings. Field-based studies, in contrast, present the ramp as dominantly composed of larger benthic foraminifera, with a carbonate production very much dependent on photozoan organisms (Condon *et al.*, 1955; Crespin, 1955; Chaproniere, 1975; Collins *et al.*, 2006). Although some studies of the exposed Miocene outcrops have been undertaken (Condon *et al.*, 1955; Crespin, 1955; Chaproniere, 1977; van de Graaff *et al.*, 1980; McNamara & Kendrick, 1994; Collins *et al.*, 2006; Riera *et al.*, 2019) integrated onshore–offshore studies are lacking that specifically address the role of environmental changes on the ramp to rimmed platform transition, or the facies architecture of the ramp at continental-margin scale.
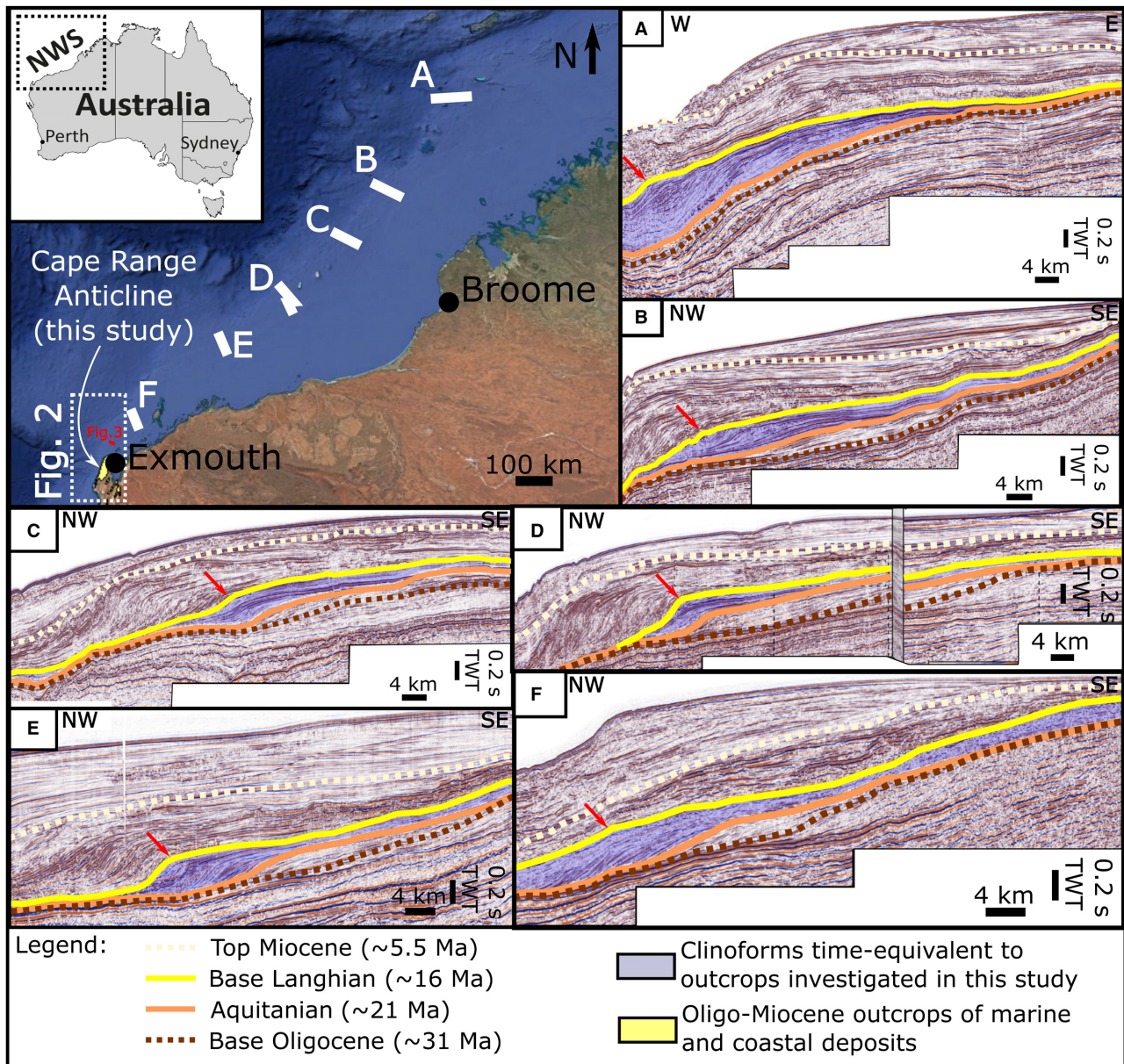
Fig. 1. Two-way travel time (TWT) seismic reflection cross-sections (A) to (F) – (A) being the northernmost section and (F) the southernmost one – along the Australian North West Shelf (NWS) showing the morphology of the continental-margin scale early Miocene ramp investigated here (seismic sections and seismic interpretations are modified after McCaffrey *et al.*, 2020). The NWS was tilted towards the south-west after 15 Ma (Sandiford, 2007), hence the slope of the ramp currently visible on seismic data is much higher than the syn-depositional early Miocene slope. The approximate location of the distal break in slope is indicated by a red arrow. This study focuses on the southernmost part of the ramp, which crops out in the Cape Range Anticline. TWT, two-way time.

This study presents an original description of the ramp exposed in the Cape Range Anticline (North West Cape) at the southern end of the NWS (Figs 1 and 2), and proposes a depositional model based on field, archived sample and cutting descriptions. The early Miocene platform reconstructed from this lithological data is then correlated with published seismic interpretations of the ramp offshore (Figs 2 and 3). The study also presents a reappraisal of marine palaeo-oceanographic conditions prevailing in the NWS during the early Miocene time interval between planktonic foraminiferal zones N5 and N7 (i.e. 21.81 to 16.4 Ma; Fig. 4; based on Blow,
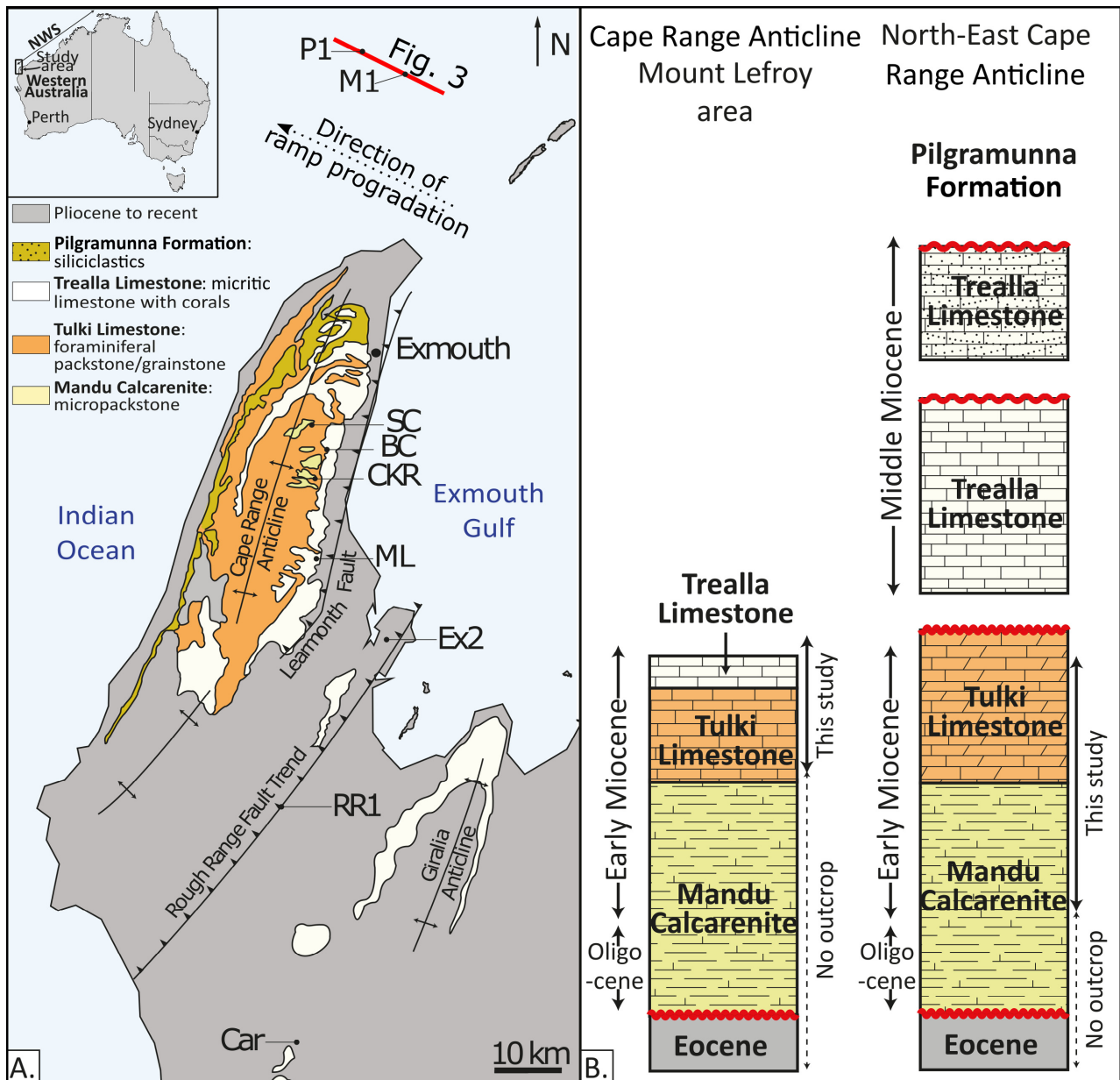
Fig. 2. (A) General geological map showing the location of the Oligo-Miocene strata cropping out in the Cape Range Anticline (modified after Condon *et al.*, 1955; Allen, 1993; Riera *et al.*, 2019) with simplified structures after Malcolm *et al.* (1991) and with location of the sections described in this study. (B) Stratigraphic columns from the eastern part of the Cape Range Anticline (modified after Condon *et al.*, 1955; Chaproniere, 1975; Riera *et al.*, 2019). Car, Cardabia 2 borehole; RR1, onshore well Rough Range South No. 1; Ex2, onshore well Exmouth No. 2; ML, Mount Lefroy; CKR, Charles Knife Road; BG, unnamed canyon north of Badjirrajirra Creek; SC, Shothole Canyon; P1, offshore well Pyrenees 1; M1, offshore well Macedon 1.

1969, and Wade *et al.*, 2011). During this early Miocene time interval, the ramp had a distally steepened to sigmoidal morphology, with no major changes in platform morphology identified. The time interval studied is equivalent to the interval OM1.5 to EMM1 (Cathro *et al.*,

2003), to the highstand Sequence N5 (Young *et al.*, 2001), and to sequences S3 (uppermost part), S4 and S5 (Riera, 2020; Fig. 3). The study was conducted in five steps: (i) fieldwork to generate outcrop descriptions, identify macroscopic fossils, analyze sedimentary structures and
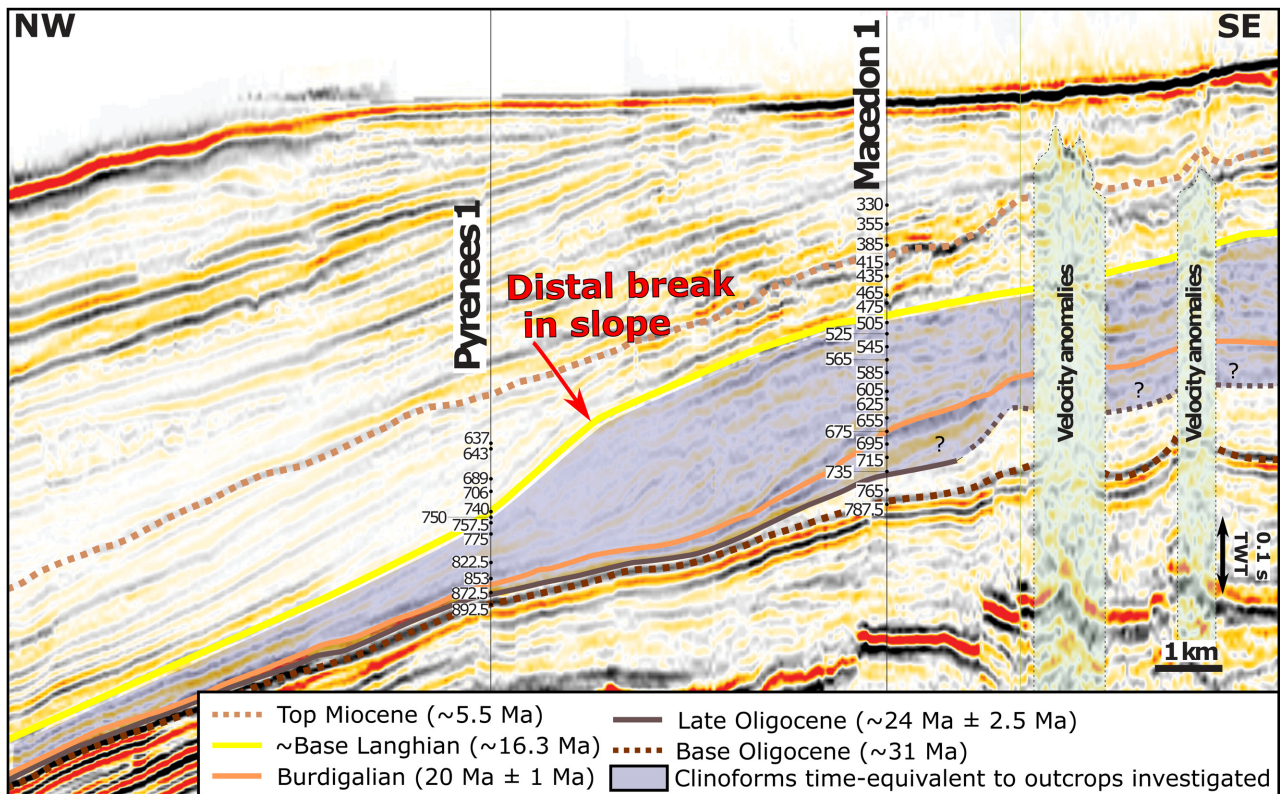
Fig. 3. Dip-oriented 2D seismic profile showing the early Miocene ramp in the vicinity of the Cape Range Anticline (section location is highlighted in red on Fig. 2; modified after Riera, 2020). The part of the ramp time-equivalent to the outcrops is highlighted in blue, while the approximate location of the distal break in slope is indicated by the red arrow.

collect representative samples; (ii) microfacies description and definition of facies and facies associations; (iii) development of a depositional model based on the spatial organization of the facies associations; (iv) correlation with seismic data; and (v) analysis of bioclast assemblages to establish the palaeoenvironmental conditions during deposition of the ramp.

GEOLOGICAL SETTING

The North West Shelf of Australia (NWS) is a continental margin formed through multiple phases of Palaeozoic and Mesozoic rifting (Veevers & Cotterill, 1978; Young *et al.*, 2001). Mesozoic and older structures were buried by thick sedimentary units by the end of the Mesozoic, and these structures have since had a limited influence on Cenozoic sedimentation, with essentially continuous sedimentation along the *ca* 2400 km long margin spanning 10° of latitude

(Apthorpe, 1988). During the Cenozoic, after the separation of Australia from Antarctica, the NWS migrated from sub-polar to tropical latitudes (Veevers & Cotterill, 1978; Young *et al.*, 2001), and evolved from a siliciclastic shelf to a carbonate margin with episodic siliciclastic influx (Apthorpe, 1988). The NWS was predominantly a passive margin during the Cenozoic, with the notable exception of its northern part which has been in a collisional phase since the Miocene (Keep *et al.*, 2007; Saqab *et al.*, 2017). In the southern part of the NWS, that is the focus of this study, isolated Mesozoic faults have been locally inverted from the Oligocene onwards (Hocking *et al.*, 1987; Cathro & Karner, 2006; Keep *et al.*, 2007). Those inversions led to the formation of the Cape Range Anticline from the Miocene onwards (van de Graaff *et al.*, 1976; Hillis *et al.*, 2008).

At the onset of the early Miocene (*ca* 23 Ma) the NWS extended from *ca* 34°S in the south (i.e. the Cape Range Anticline; Fig. 4) to *ca* 24°S

in the north (Seton *et al.*, 2012; Müller *et al.*, 2018). Seismic investigations have shown that a distally steepened carbonate ramp was present all the way along the NWS, from the northerly Browse Basin to the Exmouth Basin in the south (Apthorpe, 1988; Westphal & Aigner, 1997; Young *et al.*, 2001; Cathro *et al.*, 2003; Rosleff-Soerensen *et al.*, 2012; Anell & Wallace, 2019; McCaffrey *et al.*, 2020; Fig. 1). The NWS migrated northward with the Australian plate during the Cenozoic, and by 17 Ma its southern extent was located at *ca* 30°S (Seton *et al.*, 2012; Müller *et al.*, 2018; Fig. 4). The distal break in slope basinward of this ramp remained permanently submerged in water depth of around 100 m (Cathro *et al.*, 2003). The Miocene palaeoclimate and palaeo-oceanography of Western Australia are still debated (Fig. 4), but some studies suggest that a proto-Leeuwin current has been present along the coast of Western Australia since the Eocene (McGowran *et al.*, 1997), and that this current intensity was particularly strong during the middle Miocene (Feary & James, 1995). The early Miocene was a time of global warming (Mudelsee *et al.*, 2014), with maximum global temperatures between 17 Ma and 15 Ma, during the Miocene Climatic Optimum (MCO, Zachos *et al.*, 2001; Shevenell *et al.*, 2004; Mudelsee *et al.*, 2014; Sangiorgi *et al.*, 2018; Fig. 4). Climatically, Australia's north-western region may have been humid during the early Miocene, and arid during the middle Miocene, as indicated by the marked reduction in Western Australian palaeodrainage during the middle Miocene (Martin, 2006). The factors that led to the formation of the proto-Leeuwin current and to the middle Miocene aridification are, however, speculative, because modern oceanographic and climatic conditions are strongly related to the Pliocene constriction of the Indonesian Throughflow (Christensen *et al.*, 2017).

Onshore early Miocene strata exposed in the Cape Range Anticline that are investigated here have traditionally been mapped as three formations, namely the: (i) late Oligocene to early Miocene deep-water micropackstones of the Mandu Calcarenite; (ii) Miocene oxidized foraminiferal packstones of the Tulki Limestone; and (iii) early to middle Miocene well-cemented carbonate mudstones with corals of the Trealla Limestone (Condon *et al.*, 1955; Crespin, 1955; Chaproniere, 1975; Collins *et al.*, 2006; Riera *et al.*, 2019). In seismic-well and offshore-well studies, late Oligocene to early Miocene strata have arbitrarily been designated as Mandu Formation, Mandu Calcarenite or Tulki Limestone, whereas the middle Miocene strata are arbitrarily referred to as Trealla Formation or Trealla Limestone, with offshore facies dominantly composed of calcareous mudstones and micropackstones (Apthorpe, 1988; Romine *et al.*, 1997; Cathro *et al.*, 2003; Wallace *et al.*, 2003; Riera *et al.*, 2019).

METHOD

Fieldwork undertaken in the eastern part of the Cape Range Anticline included re-investigation of previously described canyon exposures (for example, Shothole Canyon section; Chaproniere, 1975, 1977; Collins *et al.*, 2006) and new descriptions of exposed sections in other areas (for example, Charles Knife Road, Mount Lefroy; Fig. 2A). The aim was to identify key sedimentary features and facies, and describe formation contacts where exposed. A total of 150 samples were collected and then analyzed via petrographic thin sections or acetate peels. Re-examination of archived samples was also undertaken, including: (i) rock samples collected during previous fieldwork in the Cape Range Anticline (Chaproniere, 1975; stored in the UWA Edward de Courcy Clarke Earth Science Museum at UWA); and (ii) side wall cores and cuttings from two offshore and two onshore wells, stored in the Geological Survey of Western Australia (GSWA) Perth Core Library.

Facies were designated by their macroscopic and microscopic lithological characteristics including depositional texture (Dunham, 1962), sedimentary structures and type of matrix, and biological characteristics with a particular emphasis on biogenic content, and especially larger benthic foraminifera. Emphasis was placed on the palaeo-environmental significance of selected larger benthic foraminifera (LBF) genera, because: (i) the latter are well-documented (e.g. Hallock & Glenn, 1986; Langer & Hottinger, 2000; Beavington-Penney & Racey, 2004; BouDagher-Fadel, 2018); (ii) the palaeo-environmental significance of LBF in the Miocene outcrops of the Cape Range Anticline was investigated (Crespin, 1955; Chaproniere, 1975, 1984a; Riera *et al.*, 2019), whereas no other group of Miocene organisms was investigated in detail in this area; and (iii) the terminology for the segmentation of the water column into euphotic, mesophotic and oligophotic zones
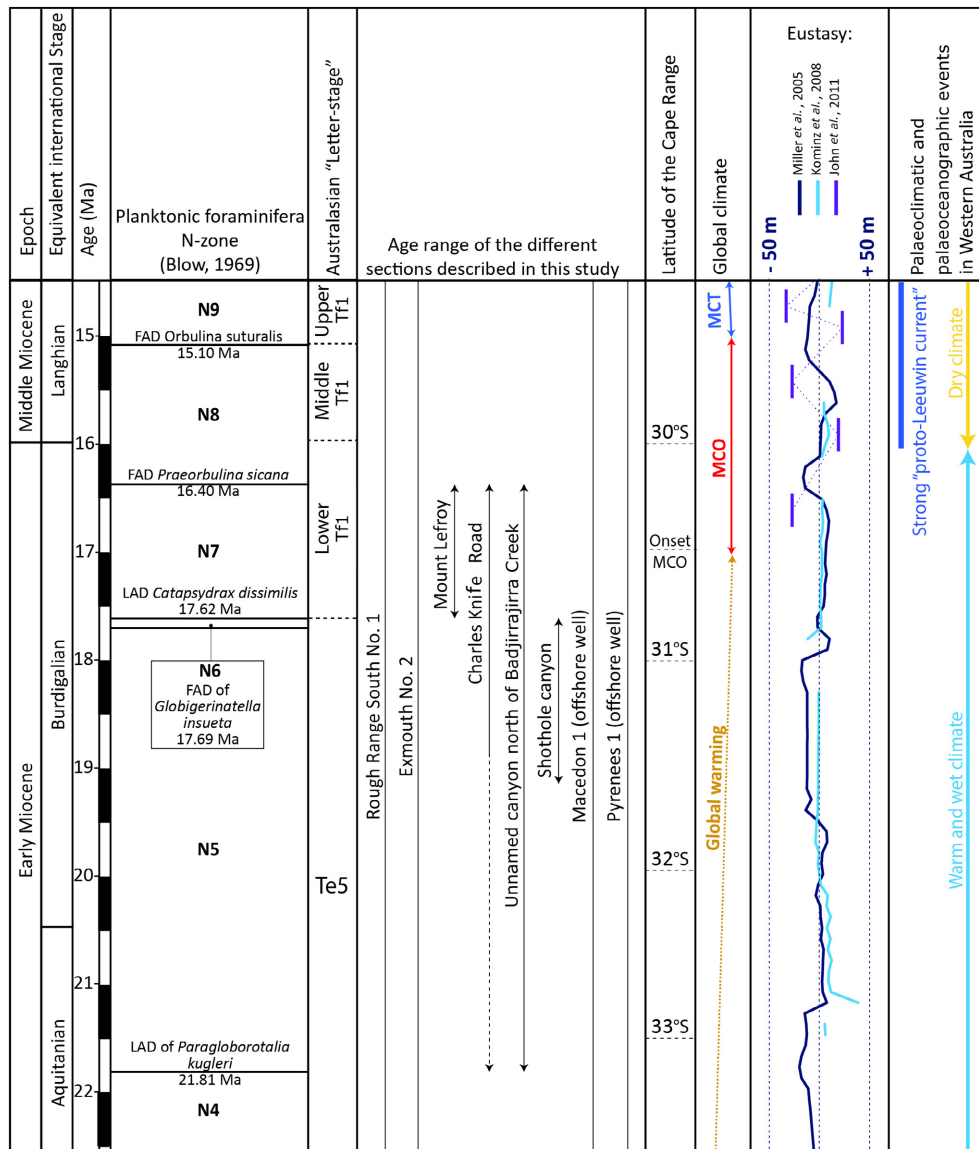
Fig. 4. Stratigraphy of the different sections described in this study including numerical timescale (Ma), chronostratigraphy (Cohen *et al.*, 2013, updated), planktonic foraminiferal N-zones (Blow, 1969, with absolute age of FAD/LAD after Wade *et al.*, 2011, table 1) and Australasian 'Letter-stages' (with absolute ages and names of Letter-stages after BouDagher-Fadel, 2018, chart 7.1). The sections are further compared with regional and global events relevant to carbonate production, including shifts in latitude, global climate, eustasy and the evolution of ocean currents and climate in Western Australia. Miocene evolution of the global climate is summarized after Flower & Kennett (1993), Zachos *et al.* (2001), Shevenell *et al.* (2004), Mudelsee *et al.* (2014) and Sangiorgi *et al.* (2018). Eustasy is after Miller *et al.* (2005), Kominz *et al.* (2008) and John *et al.* (2011). Continental climate of Western Australia is summarized after Martin (2006). Palaeo-activity of the proto-Leeuwin current is after McGowran *et al.* (1997), Wyrwoll *et al.* (2009) and O'Connell *et al.* (2012). FAD, first appearance datum; LAD, last appearance datum; Ma, million years ago; MCO, Miocene Climatic Optimum; MCT, Miocene Climate Transition.

used here follows Pomar (2001a), which itself largely builds on LBF genera occurrence and on the classification from Hottinger (1997). Hottinger's classification has been supported by recent publications (e.g. Parker & Gischler, 2015). Other organisms, such as coralline algae, were not identified at the genus level, and therefore not utilized in precise palaeoenvironmental and palaeo-water depth determinations (cf. Braga *et al.*, 2010). Some of the descriptive

terms, such as 'marl', follow terminology previously used to describe Cenozoic strata from the NWS (e.g. Apthorpe, 1988; Wallace *et al.*, 2003; Collins *et al.*, 2006). Grains present in each facies were described semi-quantitatively, with 'rare', 'common' and 'abundant' indicating <2%, 2% to 10% and >10% of the rock volume. Finally, facies were grouped into facies associations to better evaluate depositional environments.

Biostratigraphic dating and stratigraphic correlations are based on planktonic foraminifera and the LBF biostratigraphic zonations building on results from Chaproniere (1975, 1977), Crespin (1955), Rexilius & Powell (1994a,b) and Riera *et al.* (2019, Table 1). Biostratigraphic division was augmented by strontium (^{87}Sr/^{86}Sr) isotopic age dating of two outcrop samples and six offshore well samples (Table 1). ^{87}Sr/^{86}Sr ratios were normalized to an NBS 987 standard value of ^{87}Sr/^{86}Sr = 0.710235. To compare with previous studies (e.g. Rosleff-Soerensen *et al.*, 2012, 2016) a whole-rock analytical method was used. This method has been applied successfully in Oligo–Miocene carbonate platforms of the Papuan Basin (Allan *et al.*, 2000) and the Asmari Limestone from Iran (Buchem *et al.*, 2010). Strontium ages were defined based on the strontium seawater curve of McArthur & Howarth (2005), using their lookup tables calibrated to the timescales of Gradstein *et al.* (2005; Version 4: 08/03). Age error includes uncertainties in the seawater curve, analytical uncertainty and isotopic heterogeneity in the samples. Previous whole rock studies (Buchem *et al.*, 2010) indicate that, excluding larger localized outliers, age error considering all variables can be in the order of ±0.5 to 1.0 Ma.

FACIES ASSOCIATIONS

Facies Association 1 (FA-1): Marly micropackstones (aphotic zone)

Description

This monotonous facies association includes only a single facies, the marly micropackstone (Mm; Table 2), identified exclusively in well cuttings (Fig. 5A). The facies appears homogeneous in hand specimen with no grains visible. Petrographically, the fabric is composed of undifferentiated, silt-sized broken calcitic grains (i.e. micropackstone), micrite and small amounts of clay. There are also scattered silt-sized angular quartz grains (35 to 75 µm across; Fig. 5B and C). Rare biogenic components include planktonic foraminifera, millimetre-scale echinoderm debris, serpulids and hyaline foraminifera. Glauconitic grains and rare burrows have been noted.

Interpretation

Planktonic foraminifera and echinoderm debris indicate accumulation in a marine environment. The angular shape of the quartz grains suggests limited abrasion during transport, possibly reflecting a short transport to the ocean by rivers (Piller & Mansour, 1994), and then along the carbonate platform by currents (e.g. Pettijohn *et al.*, 1972). Airborne transport, however, cannot be excluded given the grain size (Rex & Goldberg, 1958; Reineck & Singh, 1980; Stuut *et al.*, 2014). Together, the presence of heterotrophic benthic organisms (i.e. small hyaline foraminifera, echinoderms, serpulids) and the absence of phototrophic benthic organisms suggest accumulation in the aphotic zone. Accumulation in a deep and aphotic environment is supported by the relative abundance of planktonic foraminifera compared to other bioclasts, and by the absence of larger foraminifera (Hallock & Glenn, 1986; BouDagher-Fadel, 2018). The scarcity of heterotrophic bioclasts (for example, rare small hyaline foraminifera), the absence of solitary corals, sponges and bivalves and the absence of phosphate may suggest accumulation in an oligotrophic environment (Lukasik *et al.*, 2000) without upwelling (see James *et al.*, 2004).

Facies Association 2 (FA-2): Silty micropackstones to rudstones (base oligophotic zone)

Description

This facies association is composed predominantly (*ca* 50%) of friable micropackstones with rare *Cycloclypeus* and scattered chert nodules (facies Mm-Cy; Table 2; Fig. 6), that distinguish it from the marly micropackstone (facies Mm of FA-1), although macroscopically they appear similar. Facies Mm-Cy also contains common small hyaline foraminifera, with rare planktonic foraminifera, serpulids, echinoderm debris and rare to abundant silt-sized angular quartz grains. The matrix is, as in the facies Mm, a micropackstone with micrite and small amounts of clay. Trace fossils are rare.

The facies Mm-Cy is typically associated with four facies (i.e. LP-Cy, Ch-Eu, Qtz-Ss, St-Eu;

Table 1. Stratigraphic markers used to calibrate the different sections described in this study. Ages are based on biostratigraphy from well completion reports (Rexilius & Powell, 1994a,b) and published material (Chaproniere, 1975, 1984a,b; Riera *et al.*, 2019) and on strontium isotope analysis.

Sections	Location on log / sample number	Letter stage (larger foraminifera)	N-zone (planktonic foraminifera)	Equivalent age (Ma)	Strontium isotope age (with Norm Ratio $^{87}Sr/^{86}Sr$)	Equivalent international stage	Based on
Rough Range South No. 1 well	158 to 220 m		N9	15.10 to 14.2 Ma	–	Langhian	Planktonic foraminifera (N-zones, Chaproniere, 1975, 1984a,b)
	220 to 310 m		N3/N4	27.5 to 21.8 Ma	–	Chattian	Planktonic foraminifera (N-zones, Chaproniere, 1975, 1984a,b)
Exmouth No 2	86 to 168 m		N9	15.10 to 14.2 Ma	–	Langhian	Planktonic foraminifera (N-zones, Chaproniere, 1975, 1984a,b)
	168 to 253 m		N3/N4	27.5 to 21.8 Ma	–	Chattian	Planktonic foraminifera (N-zones, Chaproniere, 1975, 1984a,b)
Mount Lefroy	0 to 42 m	Lower Tf1	eq. N7–(early N8)	17.62 to ˜16 Ma	–	Burdigalian	Planktonic foraminifera and larger benthic foraminifera (N-zones and letter stages, Riera *et al.*, 2019)
	42 to 67 m	Lower Tf1	N7	17.62 to 16.40 Ma	–	Burdigalian	
Charles Knife Road	0 to 21 m	Lower Tf1	late N5 to N7	17.62 to 16.40 Ma	–	Burdigalian	Planktonic foraminifera and larger benthic foraminifera (N-zones and letter stages, this study): **Larger foraminifera:** *L. Nephrolepidina (including L. (N.) ferreroi)* without *L. Eulepidina, Miogypsina, Austrotrillina, Cycloclypeus* without *Katacycloclypeus*; **Planktonic foraminifera:** *Globigerinoides trilobus* without *Globigerinoides sicanus, Praeorbulina* nor *Orbulina*
Unnamed canyon north of Badjirrajirra Creek	0 to 22 m		N5 to N7	21.8 to 16.4 Ma	–	Aquitanian (late) – Burdigalian	Planktonic foraminifera and larger benthic foraminifera (N-zones and letter stages, Chaproniere, 1975, 1984a,b)

Table 1. (continued)

Sections	Location on log / sample number	Letter stage (larger foraminifera)	N-zone (planktonic foraminifera)	Equivalent age (Ma)	Strontium isotope age (with Norm Ratio $^{87}Sr/^{86}Sr$)	Equivalent international stage	Based on
Shothole Canyon	0 to 105 m		N6	17.7 to 17.6 Ma	–	Burdigalian	Planktonic foraminifera and larger benthic foraminifera (N-zones and letter stages, Chaproniere, 1975, 1984a,b)
	38 m (MSh 8)				18.6 ± 2 Ma (0.708532)	Burdigalian	Strontium isotopes (calibration after McArthur & Howarth, 2005, this study)
	0.5 m (MSh 2)				19.2 ± 2 Ma (0.708482)	Burdigalian	Strontium isotopes (calibration after McArthur & Howarth, 2005, this study)
Macedon 1	465.0 m		N8	16.4 to 15.1 Ma	17.4 ± 2 Ma (0.708627)	Burdigalian (late) – Langhian	Planktonic foraminifera (Rexilius & Powell, 1994b) and strontium isotopes (calibration after McArthur & Howarth, 2005; this study)
	475 m		N7 or younger	17.6 Ma or younger	–	Burdigalian or younger	Planktonic foraminifera (Rexilius & Powell, 1994b)
	495 m		N6 to N7	17.7 to 16.4 Ma		Burdigalian	Planktonic foraminifera (Rexilius & Powell, 1994b)
	505 m				18.4 ± 2 Ma (0.708545)	Burdigalian	Strontium isotopes (calibration after McArthur & Howarth, 2005; this study)
	545 m		N6 to N7	17.7 to 16.4 Ma	19.0 ± 2 Ma (0.708496)	Burdigalian	Planktonic foraminifera (Rexilius & Powell, 1994b) and strontium isotopes (calibration after McArthur & Howarth, 2005; this study)
	555 m		N4 to N5	26.7 to 17.7 Ma	–	Chattian – Burdigalian	Planktonic foraminifera (Rexilius & Powell, 1994b)
	635 m		N4 to N5	26.7 to 17.7 Ma	–	Chattian – Burdigalian	Planktonic foraminifera (Rexilius & Powell, 1994b)

Table 1. (continued)

Sections	Location on log / sample number	Letter stage (larger foraminifera)	N-zone (planktonic foraminifera)	Equivalent age (Ma)	Strontium isotope age (with Norm Ratio $^{87}Sr/^{86}Sr$)	Equivalent international stage	Based on
Pyrenees 1	655 m		N4 (?)	26.7 to 21.8(?)	19.5 ± 2 Ma (0.70846)	Burdigalian	Planktonic foraminifera (Rexilius & Powell, 1994b)
	675 m		N4 (?)	26.7 to 21.8(?)	20 ± 2 Ma (0.708427)	Burdigalian	Planktonic foraminifera (Rexilius & Powell, 1994b) and strontium isotopes (calibration after McArthur & Howarth, 2005; this study)
	740 m				14.5 ± 2 Ma (0.708784)	Langhian	Strontium isotopes (calibration after McArthur & Howarth, 2005; this study)
	750 m		N8	16.40 to 15.10 Ma	–	Burdigalian (late) – Langhian	Planktonic foraminifera (Rexilius & Powell, 1994b) and strontium isotopes (calibration after McArthur & Howarth, 2005; this study)
	757.5 to 805 m		N6/N7	17.69 to 16.40 Ma	–	Burdigalian	Planktonic foraminifera (Rexilius & Powell, 1994b) and strontium isotopes (calibration after McArthur & Howarth, 2005; this study)
	822.5 to 880 m		N6/N4	26.7 to 17.62 Ma	–	Chattian – Burdigalian	Planktonic foraminifera (Rexilius & Powell, 1994b) and strontium isotopes (calibration after McArthur & Howarth, 2005; this study)
	884 m		N4	26.7 to 21.81 Ma	–	Chattian – Aquitanian	Planktonic foraminifera (Rexilius & Powell, 1994b) and strontium isotopes (calibration after McArthur & Howarth, 2005; this study)

Table 2). The latter form sub-horizontal beds interbedded with facies Mm-Cy and traceable along outcrops (Table 2; Figs 6A, 6B, 7A, 7D and 8). The laminated micropackstone with *Cycloclypeus* (facies LP-Cy; Table 2) accumulated as sub-horizontal beds, up to 10 cm thick and with erosional bases (Figs 6B, 7A and 8C). Centimetre-scale fragments of branching bryozoans and echinoderms are very rarely present in the lower parts of the beds. Petrographic observations reveal that beds are normally graded and dominantly composed of laminated bioclastic foraminiferal packstones at their bases and foraminiferal wackestones at their tops. The facies (LP-Cy) contains laminae with concentrated fragmented bioclasts, such as *Cycloclypeus*, *Lepidocyclina* *(Nephrolepidina)*, serpulids, echinoderm debris and coralline algae, particularly in the basal packstones. The matrix is a micropackstone with micrite.

The chaotic *Eulepidina* rudstone (facies Ch-Eu; Table 2) is characterized by metre-thick beds with a monospecific assemblage of *Lepidocyclina (Eulepidina) badjirraensis* randomly arranged in a clast-supported fabric with micropackstone and micrite matrix (Figs 7A, 7C and 8D). *L. (E.) badjirraensis* tests have diameters between 0.5 cm and 2.0 cm, and they are 0.5 mm thick. Beds of this facies commonly have erosional bases. The facies is homogeneous and does not change in composition from base to top.

The very fine quartz sandstone (facies Qtz-Ss; Table 2) is exclusively composed of fine, angular and well-sorted quartz grains. Bed thicknesses range from 5 to 15 cm, and the bases of the beds are erosional (Figs 6B, 8A and 8B).

The stacked *Eulepidina* rudstone (facies St-Eu, Table 2) forms beds up to 5 cm thick with planar bed bases and is characterized by a high density of complete *Lepidocyclina (Eulepidina) badjirraensis* tests. Foraminifera are densely stacked in assumed life position, and they were found to support a rare although diverse encrusting cheilostome bryozoan fauna (Figs 7D, 7E and 8B). Matrix is a micropackstone with micrite.

Interpretation
The stenohaline biota in these facies are indicative of marine conditions. In the marly micropackstone with rare *Cycloclypeus* (Mm-Cy), the sparsity of fragmented *Cycloclypeus* and the absence of other phototrophic organisms suggest that deposition took place at or near the base of the oligophotic zone. This is based on *Cycloclypeus* usually living in calm waters at the base of the photic zone (Hottinger, 1997; Beavington-Penney & Racey, 2004; Riera et al., 2019). The laminated micropackstone with *Cycloclypeus* (LP-Cy) is interpreted as a waning flow deposit based on normal grading, even if type of flow could not be traced. Moreover, the facies LP-Cy contains a mix of fragmented organisms, comprising phototrophic as well as heterotrophic taxa concentrated in thin laminae which, together, are consistent with downslope transport of sediment produced in the oligophotic zone. The presence of giant forms of *Eulepidina* have elsewhere been interpreted as an indicator of a low-energy, oligophotic and oligotrophic environment (Hallock & Glenn, 1985; Renema & Troelstra, 2001; Pomar et al., 2017). The presence of complete tests of *Lepidocyclina (Eulepidina) badjirraensis* in the stacked *Eulepidina* rudstone (St-Eu) is here interpreted as an indication of *in situ* accumulation with *Eulepidina* in life position. The absence of quartz in this facies (St-Eu) further suggests that *L. (E.) badjirraensis* were periodically colonising the lower part of the oligophotic zone when influx of quartz was minimal. In the chaotic *Eulepidina* rudstone (Ch-Eu), the absence of photozoan organisms other than the giant thin and flat *L. (E.) badjirraensis* is interpreted as an indication of production towards the base of the photic zone because of their flat and large tests (Hottinger, 1997; Beavington-Penney & Racey, 2004). The lack of orientation of those tests may indicate episodic higher energy events (such as marine currents, internal waves, storm waves) affecting only the very base of the photic zone. The very fine, angular grains dominating the laminated quartz sandstone (Qtz-Ss) are most likely derived from terrestrial environments by rivers or wind, and they were possibly redistributed in the water column by currents or storms, before being accumulated on the seafloor. Overall, FA-2 is interpreted as having accumulated at the base of the oligophotic zone, with facies Mm-Cy representing the combined background accumulation of pelagic and bioclastic debris, intermittently interrupted by higher energy flow deposits produced by storms and/or carried by currents. Only facies St-Eu stands out, possibly indicating intervals of high benthic phototrophic production in the deepest part of the oligophotic zone, during calmer periods when siliciclastic influx was minimal and the water column potentially depleted in nutrients (i.e. oligotrophic). Finally, the chaotic *Eulepidina*

Table 2. Components of sedimentary facies and facies associations identified in the early Miocene ramp investigated.

Facies association	Facies	Short name	Grains (macroscopic)	Grains (microfacies)	Bioturbations/ sedimentary structures	Matrix	Depositional environment
FA-1: Marly micropackstones of the aphotic zone	Marly micropackstone	Mm	/	r. planktonic foraminifera, r. millimetre-scale echinoderm debris, r. serpulids, r. hyaline foraminifera, r. glauconite grains, c. fine angular quartz	v. r. burrows	Micropackstone and micrite, small amount of clay	Aphotic zone, oligotrophic environment
FA-2: Silty micropackstones to rudstones of the base of the oligophotic zone	Marly micropackstone with rare *Cycloclypeus*	Mm-Cy	r. chert nodules (sponges?)	c. small hyaline foraminifera, r. planktonic foraminifera, r. broken *Cycloclypeus*, r. serpulids, r. echinoderm debris and r. to a. very well-sorted fine angular quartz grains	r. burrows	Micropackstone and micrite, small amount of clay	Lowermost part oligophotic zone, warm oligotrophic marine waters, predominantly calm with occasional higher energy events driven by internal waves, currents and storms
	Micropackstone with *Cycloclypeus*	LP-Cy	v.r. br. branching bryozoans, vr. r. echinoderm fragments	r. broken *Cycloclypeus*, r. *Lepidocyclina (Nephrolepidina)*, r. broken serpulid, r. broken echinoderm debris and r. broken articulated coralline algae	erosive base, laminated, thinning upward	Micropackstone and micrite	
	Chaotic *Eulepidina* rudstone	Ch-Eu	*Lepidocyclina (Eulepidina) badjirraensis*		erosive base, chaotic	Micropackstone and micrite	
	Very fine quartz sandstone	Qtz-Ss	/	Fine angular quartz	erosive base, laminated	?	
	Stacked Eulepidina rudstone	St-Eu	a. *Lepidocyclina (Eulepidina) badjirraensis*, v. r. encrusting bryozoans		stacked horizontal organism (living position)	Micropackstone and micrite	
FA-3: Wackestones–packstones with flattened Rotaliida of the oligophotic zone	Wackestone with *Eulepidina* and *Operculina*	Wa-Eu	/	r. to c. entire *Cycloclypeus*, r. entire *Lepidocyclina (Eulepidina) badjirraensis*, v.r. *Operculina*, v.r. *Amphistegina*, r. to a. small hyaline foraminifera, r. to c. planktonic foraminifera, r. bryozoans, r. echinoderm debris, r. to a. fine angular quartz grains	/	Micropackstone and micrite	Oligophotic zone, warm marine waters with constant *in situ* reworking and mixing by swell, storms, internal tides and/or infaunal organism

Table 2. (continued)

Facies association	Facies	Short name	Grains (macroscopic)	Grains (microfacies)	Bioturbations/ sedimentary structures	Matrix	Depositional environment
	Packstone–floatstone with *Cycloclypeus* and *Nephrolepidina*	Pa-Cy	r. entire irregular echinoid tests, v.r. bivalves	c. to a. entire and fragmented *Cycloclypeus*, c. entire *Operculina*, r. entire flattened *Lepidocyclina (Nephrolepidina)*, r. to c. *Lepidocyclina (Eulepidina)*, v. r. *Sphaerogypsina*, r. to a. small hyaline foraminifera, v.r. small miliolids, r. to c. planktonic foraminifera, and r. to a. articulated coralline algae, r. to c. bryozoans, r. echinoderm debris, r. to c. fine angular quartz grains	locally heavily burrowed	Micropackstone and micrite	
	Laminated packstone–floatstone with *Cycloclypeus* and *Nephrolepidina*	La-Cy	v.r. bivalves	c. to a. entire and broken *Cycloclypeus*, c. to a. entire and broken flattened *Lepidocyclina (Nephrolepidina)*, v.r. Soritids, r. to a. small hyaline foraminifera, v.r. small miliolids, r. to c. planktonic foraminifera, v.r. green algae, r. to a. articulated coralline algae, r. to c. bryozoan, r. serpulids, r. echinoderm debris and a. very fine angular quartz grains	bedding, *Cycloclypeus* and *Lepidocyclina (N.)* are parallel to each other	Micropackstone and micrite	
	Peloidal grainstone with hyaline foraminifera	Gr-Pe	v.r. bivalves	a. peloids, c. small hyaline foraminifera, r. to c. planktonic foraminifera, v.r. coralline algae, and c. echinoderm debris	/	/	
FA-4: Wackestones–grainstones with robust Rotalida of the mesophotic zone	Wackestone–grainstone with *Nephrolepidina*, *Cycloclypeus* and coralline algae	Gr-Ne	r. large bivalve shells, r. broken irregular echinoderms, r. encrusting coralline algae, v. r. corals and r. gastropods	r. to a. peloids, microbored large rotaliids (r. to a. *Cycloclypeus*, r. to a. *Operculina*, r. to a. juveniles and adults *Lepidocyclina (Nephrolepidina)*), v.r. to r. Soritids, v.r. *Austrotrillina*, r. to a. encrusting coralline algae, c. articulated coralline algae, r. to c. acervulinids including *Miogypsina*, *Acervulina* and *Sphaerogypsina*, r. agglutinated foraminifera, r. small hyaline foraminifera, r. to c. green algae, r. to c. small miliolids, r. planktonic foraminifera, r. to c. echinoderm debris, r. to c. bryozoans	LBF are microbored and oxidized (whereas matrix is not oxidized)	Micrite	Mesophotic zone, energetic open-marine condition, strong action of swell and storm-waves on the seafloor

Table 2. (continued)

Facies association	Facies	Short name	Grains (macroscopic)	Grains (microfacies)	Bioturbations/sedimentary structures	Matrix	Depositional environment
FA-5: Wackestones–grainstones with Miliolida and Rotaliida of the uppermost mesophotic zone	Wackestone–grainstone with *Nephrolepidina* and coralline algae	Gr-Mi	v.r. to a. coralline algae, r. bivalves and v.r. corals	r. to a. peloids, porcelaneous foraminifera (r. to c. *Flosculinella*, r. to c. *Austrotrillina*, and r. to c. *Sorites*), Rotaliids foraminifera (r. *Lepidocyclina* (*Nephrolepidina*)), r. to c. *Operculina*, r. small miliolids, r. to c. broken articulated algae, r. to a. encrusting coralline algae, r. to c. acervulinids with flat or circular shapes, r. to c. *Sphaerogypsina*, r. to c. green algae, r. to c. echinoderm debris, r. to c. bryozoans	/	Micrite	Uppermost mesophotic zone, muddy bottom, winnowing, oligotrophic, possible high hydrodynamic stress, sparse seagrass meadows

v.r., very rare; r., rare; c., common; a., abundant; LBF, Larger Benthic Foraminifera.

rudstone (Ch-Eu) could indicate sediment reworking at the base of the oligophotic zone interpreted as the effect of currents, perhaps due to the presence of internal waves (e.g. Pomar *et al.*, 2012). Thus, FA-2 is interpreted as deposited in an overall calm environment, affected episodically by high energy events.

Facies Association 3 (FA-3): Wackestones–packstones with flattened Rotaliida (oligophotic zone)

Description
This facies association is composed of four facies, attaining a combined thickness of at least 100 m in individual outcrops (Table 2; Figs 9 to 11). The wackestone–floatstone with *Eulepidina* and *Operculina* (facies Wa-Eu; Table 2; Figs 9A, 9B and 11) contains randomly organized bioclasts, rare to abundant fine angular quartz grains and no sedimentary structures. The matrix of facies Wa-Eu is dominated by micropackstone and micrite similar to that in facies Mm and Mm-Cy (Fig. 9B). Bioclasts include rare to common complete *Cycloclypeus*, rare complete *Lepidocyclina* (*Eulepidina*) *badjirraensis,* and very rare *Operculina* and *Amphistegina*, as well as rare to abundant small hyaline foraminifera, rare to common planktonic foraminifera, rare bryozoans and rare echinoderm debris.

The packstone with *Cycloclypeus* and *Sphaerogypsina* (facies Pa-Cy; Table 2) is a poorly to well-cemented, beige to orange limestone. It is locally bioturbated and contains rare complete irregular echinoid tests (Figs 9D and 10B) and very rare bivalves. The matrix is composed of micropackstone and micrite with rare to common fine angular quartz grains (Fig. 9E). Biogenic material includes common to abundant complete or fragmented *Cycloclypeus*, common complete *Operculina*, rare complete flat *Lepidocyclina* (*Nephrolepidina*), rare to common complete *Lepidocyclina* (*Eulepidina*), very rare *Sphaerogypsina*, rare to abundant small hyaline foraminifera, very rare small miliolids, rare to common planktonic foraminifera as well as rare fragments of articulated coralline algae, and rare to common bryozoan and rare echinoderm debris.

The laminated packstone–floatstone with *Cycloclypeus* (facies La-Cy; Table 2) is characterized by oblique parallel lamination. The facies was identified at a single locality (Figs 10C and 11). The matrix is a micropackstone with micrite and abundant angular very fine quartz grains
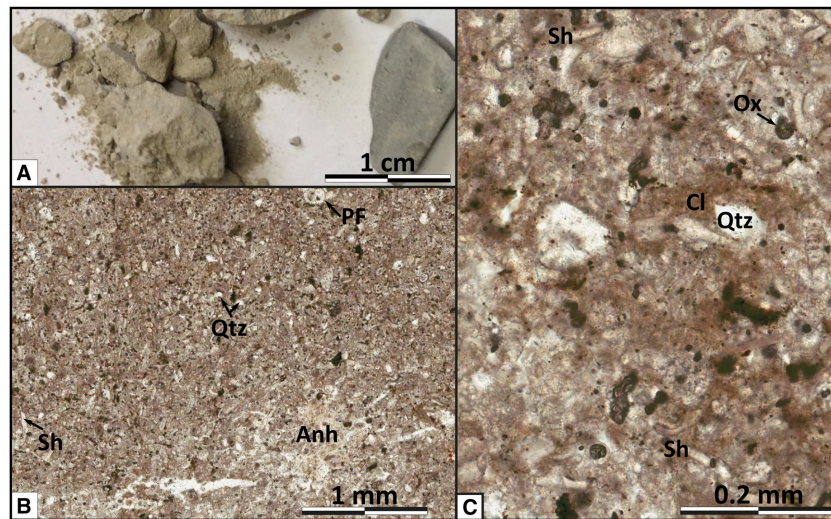
Fig. 5. Photographs of the single facies forming Facies Association 1 (FA-1), the facies marly micropackstone (Mm), at different scales of observation. (A) Photograph of a ditch cutting from the offshore well Pyrenees 1 (sample collected at 775mRT). (B) Photomicrograph of the thin section of the same ditch cutting (plane-polarized light, Pyrenees 1-775mRT) highlighting the presence of quartz grains (Qtz), shell debris (Sh), planktonic foraminifera (PF) and anhydrite (Anh). (C) Higher magnification photomicrograph of the same thin section (plane-polarized light, Pyrenees 1-775mRT) showing the microstructure of facies Mm and highlighting the presence of very fine shell debris (Sh), oxides (Ox), clayey matrix (Cl) and quartz grains (Qtz).
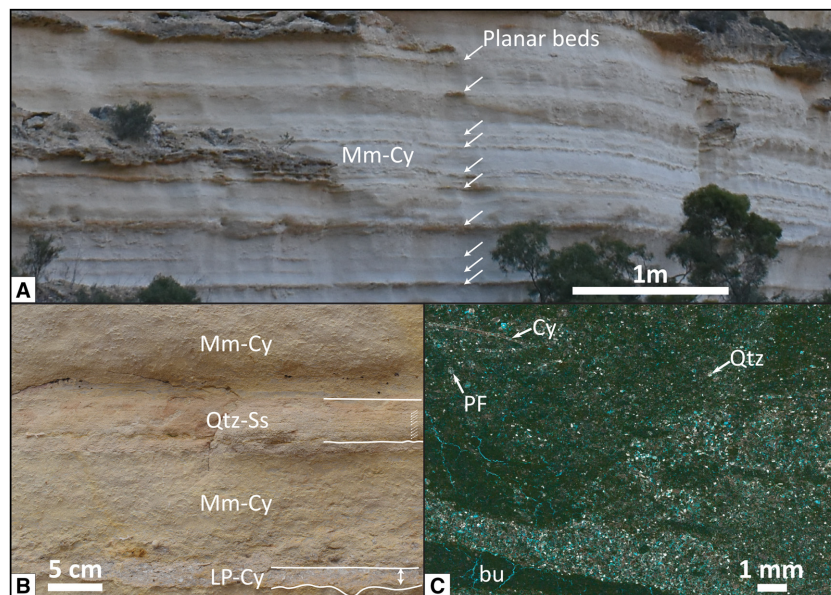

Fig. 6. Outcrop photographs and photomicrographs of the facies marly micropackstone with rare *Cycloclypeus* (Mm-Cy, from the facies association FA-2). (A) Outcrop photograph illustrating the alternation of facies Mm-Cy and of planar beds in the lower part of the Shothole Canyon section. (B) Close-up outcrop view of the alternation of facies Mm-Cy and planar beds of laminated quartz sandstone (facies Qtz-Ss; laminae are indicated by slanted arrows) and laminated packstone–floatstone with *Cycloclypeus* (facies LP-Cy) at the base of the Shothole Canyon section. (C) Photomicrograph of the facies Mm-Cy (plane-polarized light) showing the matrix made of clayey micropackstone, and highlighting the presence of *Cycloclypeus* (Cy), planktonic foraminifera (PF), quartz grains (Qtz) and burrows (bu).

distributed homogeneously (Fig. 10D). The bioclastic content is dominated by complete and fragmented flat, and commonly imbricated, tests of *Cycloclypeus* and *Lepidocyclina (Nephrolepidina)*. Other grains include very rare soritids, rare to abundant small hyaline foraminifera, very rare small miliolids, rare to common planktonic foraminifera, very rare green algae, rare to abundant articulated coralline algae, rare to common bryozoans, rare serpulids and rare echinoderm debris.

The peloidal grainstone with hyaline foraminifera (facies Gr-Pe; Table 2) was also identified only at a single outcrop, covered with modern desert varnish. The only macroscopic grains identified are very rare bivalves. Petrographic observation shows that facies Gr-Pe has a clast-supported fabric, with grains dominantly composed of abundant peloids, common small hyaline foraminifera, rare to common planktonic foraminifera, very rare coralline algae and common echinoderm debris (Fig. 10E).
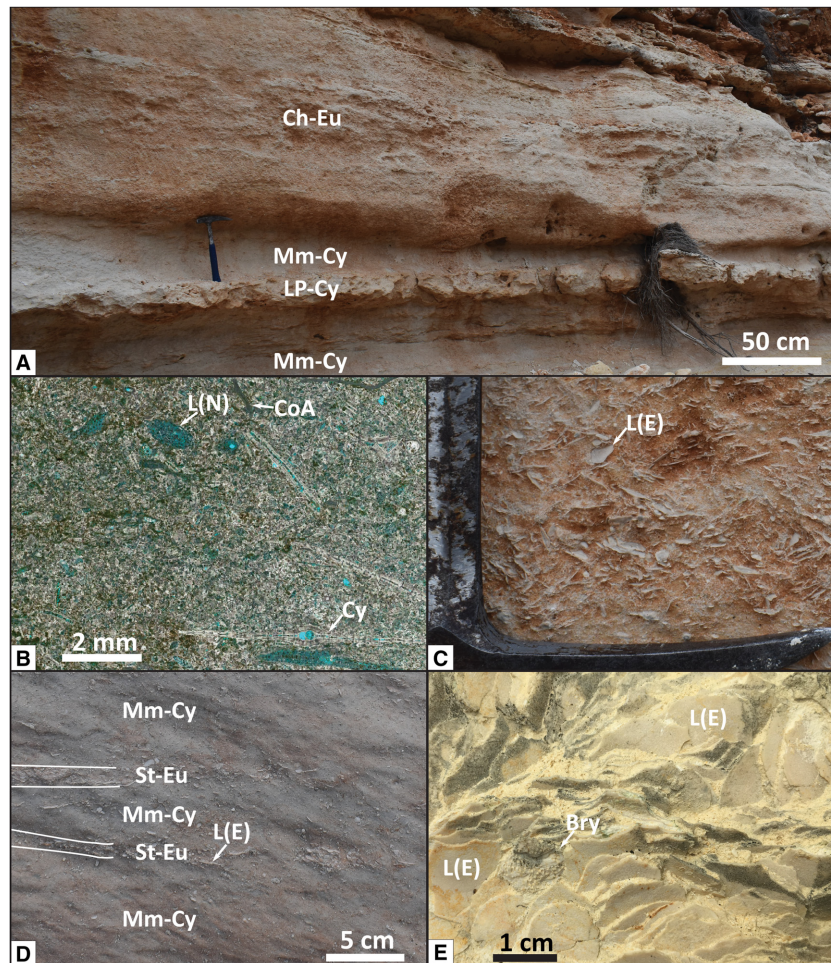

Fig. 7. Outcrop photographs and photomicrographs of different facies from Facies Association 2 (FA-2). (A) Outcrop photograph showing a massive bed of chaotic *Eulepidina* rudstone (facies Ch-Eu) overlying marly micropackstone with rare *Cycloclypeus* (facies Mm-Cy) and a thin bed of laminated packstone−floatstone with *Cycloclypeus* (facies LP-Cy) in the unnamed canyon north of Badjirrajirra Creek. (B) Photomicrograph of a thin section (plane-polarized light) of the laminated micropackstone with *Cycloclypeus* (facies LP-Cy) from the lower part of the Shothole Canyon section (sample Msh3). (C) Close-up outcrop photograph of the chaotic *Eulepidina* rudstone (facies Ch-Eu). (D) Thin beds of stacked *Eulepidina* rudstones (facies St-Eu) embedded in the marly micropackstone with rare *Cycloclypeus* (facies Mm-Cy). (E) Close-up view of a sample with stacked *Eulepidina* rudstone (facies St-Eu), note the presence of rare encrusting bryozoans on the *Lepidocyclina (Eulepidina)* tests. Bry, bryozoan; CoA, coralline algae; Cy, *Cycloclypeus*; L(E), *Lepidocyclina (Eulepidina)*; L(N), *Lepidocyclina (Nephrolepidina)*.
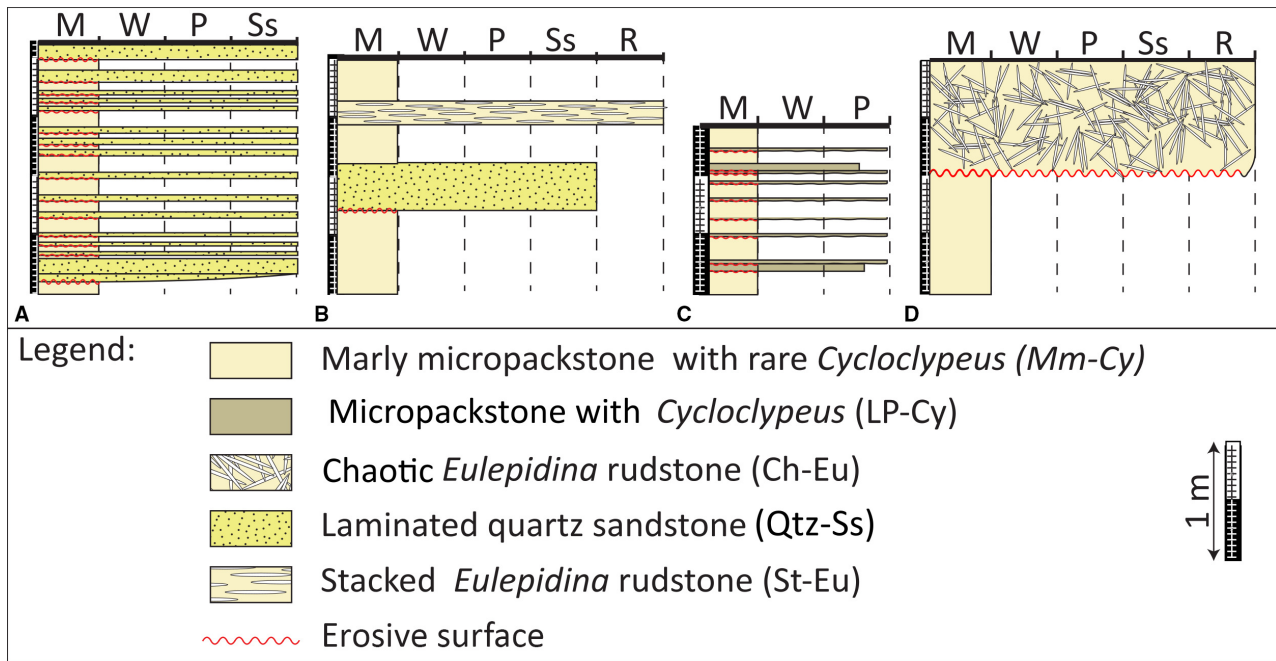
Fig. 8. Detail of the different types of vertical organization of FA-2 at the base of the Shothole Canyon section (A) to (C) and from the BC section (D). (A) Alternation of marly micropackstone with rare *Cycloclypeus* (facies Mm-Cy) and laminated quartz sandstone (facies Qtz-Ss). (B) Facies Mm-Cy intersected by a thick bed of laminated quartz sandstone (facies Qtz-Ss), note the presence of a stacked *Eulepidina* rudstone (facies St-Eu) in the upper part of the section. (C) Alternation of facies Mm-Cy with thin beds of laminated packstone–floatstone with *Cycloclypeus* (LP-Cy) having erosive bases. (D) Facies Mm-Cy overlain by a thick bed of chaotic *Eulepidina* rudstone (facies Ch-Eu) with an erosive base. M, mudstone; W, wackestone; P, packstone; Ss, siliciclastic; R, rudstone.

Interpretation

The wackestone–floatstone with *Eulepidina* and *Operculina* (Wa-Eu) contains a foraminiferal assemblage (i.e. *Cycloclypeus, Lepidocyclina (Eulepidina) badjirraensis, Operculina* and *Amphistegina*) typical of the oligophotic zone of warm oceans (Hallock, 1987; Hottinger, 1997; Pomar, 2001a; Renema & Troelstra, 2001; Beavington-Penney & Racey, 2004; Pomar *et al.*, 2017). The good preservation and random orientation of the dominating flat and fragile foraminiferal tests suggests limited mechanical and/or biological reworking, with possibly dominantly *in situ* mixing (Beavington-Penney *et al.*, 2005). The absence of organisms characteristic of the euphotic and mesophotic zones (such as *Austrotrillina*, soritids, alveolinids and miogypsinids; Hottinger, 1997; Beavington-Penney & Racey, 2004) may further indicate that downslope transport of sediment was minimal during deposition of this facies. The packstone with *Cycloclypeus* and *Nephrolepidina* also contains a foraminiferal assemblage characteristic of the oligophotic zone [i.e. *Cycloclypeus, Operculina* and flat *Lepidocyclina (Nephrolepidina)*;

Hottinger, 1997; Pomar, 2001a,b; Beavington-Penney & Racey, 2004] together with *Sphaerogypsina* and fragments of articulated coralline algae. This assemblage indicates sediment accumulation at shallower depths than that of facies Wa-Eu. The preservation of complete tests of irregular echinoids suggests that physical disturbance was of moderate intensity, affecting only the surficial layers of sediment (Mancosu & Nebelsick, 2017). The laminated packstone–floatstone with *Cycloclypeus* (La-Cy) may be associated with currents bearing suspended quartz grains, possibly due to increased river runoff after major storms or cyclones. The foraminiferal assemblage present in La-Cy [i.e. *Cycloclypeus* and *Lepidocyclina (Nephrolepidina)*] suggests a sediment source in the oligophotic zone (Hottinger, 1997; Pomar, 2001a; Beavington-Penney & Racey, 2004). The fine peloids in the peloidal grainstone with hyaline foraminifera (Gr-Pe) could be reworked from a more proximal part of the platform. FA-3 is interpreted as accumulated in an overall calm environment affected episodically by high energy events, but in a shallower setting than FA-2.

Facies Association 4 (FA-4): Wackestones–grainstones with robust Rotaliida (mesophotic zone)

Description

This facies association includes only a single facies: a wackestone–grainstone with *Nephrolepidina*, *Cycloclypeus* and coralline algae (facies Gr-Ne; Table 2; Fig. 12). In outcrop, this facies is a massive, well-cemented pale-coloured white to orange limestone with a desert varnish coating (Table 2; Fig. 12A). Rare irregular echinoids are present in this facies but, unlike facies Pa-Cy (FA-3), they are commonly fragmented. Macroscopically, facies Gr-Ne further differs from facies Pa-Cy in containing rare bivalve shells (Fig. 12B), rare encrusting coralline algae, rare gastropods and very rare corals. Petrographic observations showed that abundant bioclastic fragments are either oxidized with microboring, or pristine. Bioclasts include large rotaliids (rare to locally abundant *Cycloclypeus*, rare to abundant *Operculina*, rare to abundant juvenile and adult *Lepidocyclina (Nephrolepidina)* including rare *L. (N.) ferreroi*), very rare to rare soritid*s*, very rare *Austrotrillina,* rare to abundant encrusting coralline algae, common articulated coralline algae, rare to common acervulinids including *Acervulina*, common *Miogypsina*, common *Sphaerogypsina*, rare agglutinated foraminifera, rare small hyaline foraminifera, rare planktonic foraminifera, rare green algae, rare to common small miliolids, rare to common bryozoans and rare to common echinoderm debris. Where present, the matrix is composed of micrite (Fig. 12C to E).

Interpretation

The foraminiferal assemblage (characterized by *Sphaerogypsina*, *Cycloclypeus* and diverse *Lepidocyclina (Nephrolepidina) including L. (N.) ferreroi*) of this facies is typically associated with warm, high-energy open-marine conditions in the mesophotic zone (Hottinger, 1997; Boudagher-Fadel & Lord, 2000; Pomar, 2001a; Beavington-Penney & Racey, 2004; Hallock & Pomar, 2008; BouDagher-Fadel, 2018). In particular, massive pillars in *L. (N.) ferreroi* and the robust morphology of *Lepidocyclina (Nephrolepidina)* are often interpreted as indicative of a high-energy marine environment (Boudagher-Fadel & Lord, 2000; Hallock & Pomar, 2008; BouDagher-Fadel, 2018). However, the presence of micrite suggests that wave agitation on the seafloor was not constant. The abundance of microspheric forms of *Lepidocyclina* suggests deposition in optimal water depths for this genus (around 40 to 80 m; Hottinger, 1997; equivalent to the mesophotic zone of Pomar, 2001a). The rare presence of soritids and *Austrotrillina* may indicate occasional reworking of grains from the euphotic zone (Hottinger, 1997; Beavington-Penney & Racey, 2004). The abundance of juvenile *Lepidocyclina* point to high juvenile mortality, which, together with the reduced size and more robust tests of larger foraminifera [for example, *L. (N.) ferreroi* and of *Sphaerogypsina*; Fig. 12E] when compared with Facies Associations 2 and 3, point to less stable environmental conditions, punctuated by high energy events such as storms (Hallock, 1985; Beavington-Penney & Racey, 2004). The thick crust of desert varnish prevented observation of sedimentary structures (such as hummocky cross-stratification and graded beds) which would support this interpretation.

Facies Association 5 (FA-5): Wackestones–grainstones with Miliolida and Rotaliida (uppermost mesophotic zone)

Description

This facies association comprises just a single facies (facies Gr-Mi; Table 2) that is only recorded in archived material (Fig. 13). The facies is a peloidal wackestone to grainstone with porcelaneous foraminifera (Fig. 13A) and locally abundant coralline algae (Fig. 13B). No sedimentary structures were identified in the archived samples, and the absence of field observations prevent any conclusions on large-scale sedimentary structures. The facies is quartz-free and, in addition to the porcelaneous foraminifera (i.e. rare to common *Flosculinella*, rare to common *Austrotrillina* and rare to common *Sorites*), this facies yields Rotaliid foraminifera [i.e. rare *Lepidocyclina (Nephrolepidina)*, rare to common *Operculina*], rare small miliolids, rare to common broken articulated algae, rare to abundant encrusting coralline algae, rare broken unarticulated coralline algae, rare to common acervulinids with flat or circular shapes, rare to common *Sphaerogypsina*, rare to common green algae, rare to common echinoderm debris and rare to common bryozoan fragments (Fig. 13C and D). Coralline algae are locally encrusted by acervulinids. Where present, the matrix is composed of micrite (Fig. 13C).

Fig. 9. Outcrop photographs and photomicrographs of the facies in Facies Association 3 (FA-3) in the central part of the Shothole Canyon section. (A) Outcrop photograph of wackestone–floatstone with *Eulepidina* and *Operculina* (facies Wa-Eu), close-up shows a *Cycloclypeus* in inferred living position. (B) Photomicrograph of the facies Wa-Eu (plane-polarized light), highlighting the presence of pristine and complete tests of *Cycloclypeus* (Cy), *Lepidocyclina (Eulepidina)* (L(E)), *Operculina* (Op) and *Amphistegina* (Am). (C) Outcrop photograph of the packstone with *Cycloclypeus* and *Sphaerogypsina* (facies Pa-Cy), note the presence of two echinoid spines (Ec) and of a bivalve shell (Bi). (D) Outcrop photograph of the facies Pa-Cy showing a horizontal burrow (Bu) and a test of an irregular echinoid (IE). (E) Photomicrograph of the facies Pa-Cy (plane-polarized light), highlighting the abundance of *Cycloclypeus* tests (Cy) and the presence of *Lepidocyclina (Nephrolepidina)* (L(N)), tests are both pristine (Pri) and bioeroded (BioE).
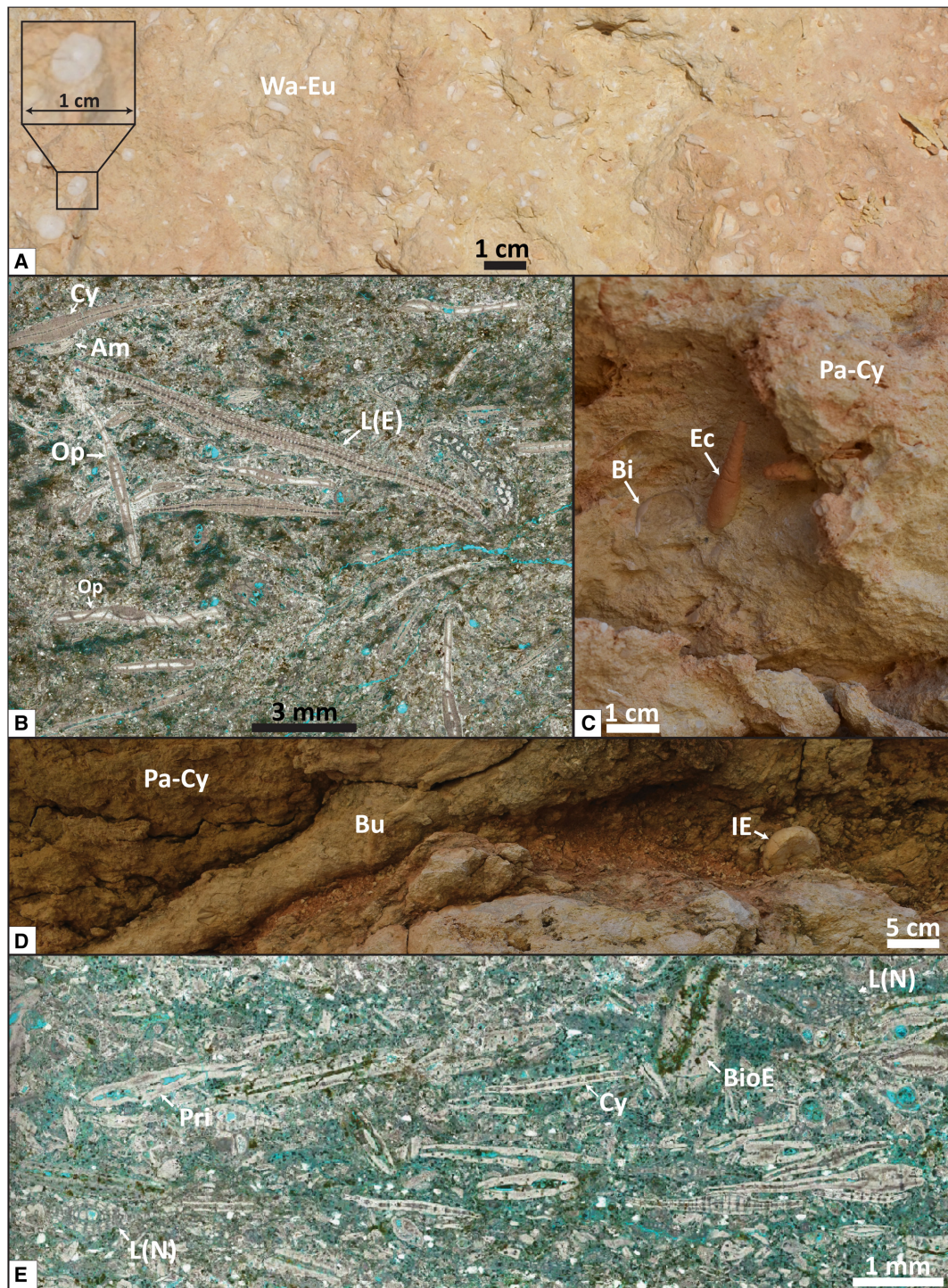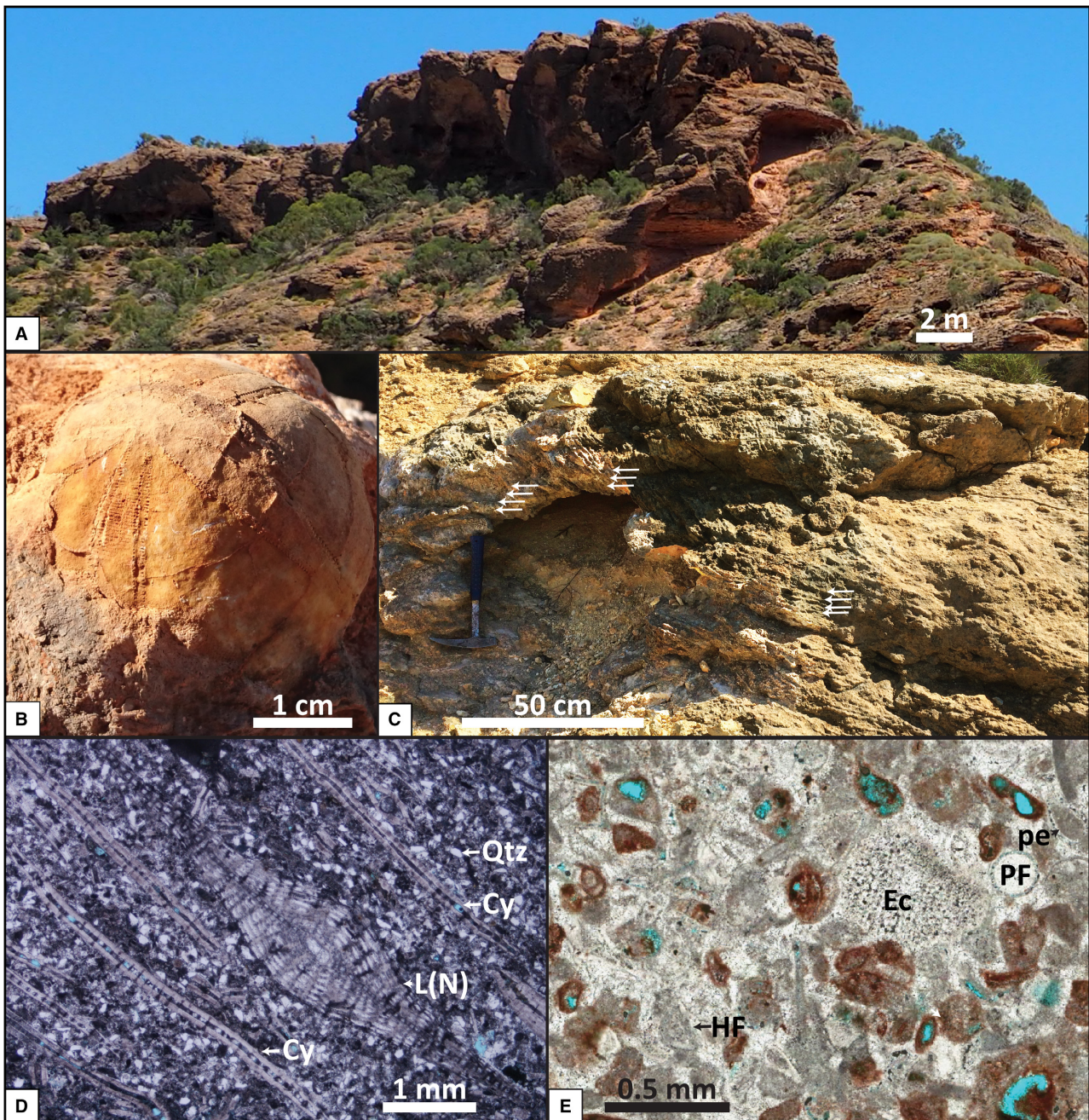
Fig. 10. Outcrop photographs and photomicrographs of the facies from Facies Association 3 (FA-3) in the upper part of the Shothole Canyon section. (A) Outcrop photograph showing the packstone with *Cycloclypeus* and *Sphaerogypsina* (facies Pa-Cy) in the upper part of the Shothole Canyon section. (B) Complete test of an irregular echinoid referred to *Conoclypus westraliensis* (following identification by Crespin, 1944) embedded in the facies Pa-Cy. (C) Cross-bedding in the packstone with *Cycloclypeus* and *Nephrolepidina* (facies Pa-Ne) in the upper part of the Shothole Canyon section; bedding is indicated by white arrows. (D) Photomicrograph of a thin section of the laminated packstone−floatstone with *Cycloclypeus* and *Nephrolepidina* (facies Pa-Ne, plane-polarized light, sample MSH10), note that the tests of *Lepidocyclina (Nephrolepidina)* (L(N)) and of *Cycloclypeus* (Cy) are parallel to one another, and that there is a high quartz (Qtz) content in the matrix. (E) Photomicrograph of the peloidal grainstone with hyaline foraminifera (facies Gr-Pe, plane-polarized light), highlighting the presence of peloids (pe), hyaline foraminifera (HF), echinoderm debris (Ec) and planktonic foraminifera (PF).

Interpretation

The presence of stenohaline organisms is indicative of accumulation in an open marine environment. The presence of large Miliolida (i.e. *Flosculinella*, *Austrotrillina*), epiphytic *Sorites*, miliolids and green algae together with coralline algae in the absence of *Cycloclypeus* suggests deposition in relatively shallow waters, while the presence of *Lepidocyclina* indicates accumulation in an environment not shallower than the upper part of the mesophotic zone, at about 40 m water depth (Langer & Hottinger, 2000; Beavington-Penney & Racey, 2004). The shape of the acervulinids matches the shape of seagrass leaves and stems, indicating the presence of sparse seagrass meadows. Robust forms of *Lepidocyclina (Nephrolepidina)* with pillars, including *L. (N.) ferreroi* (Fig. 13C), and of *Sphaerogypsina* may indicate that FA-5 accumulated in a high-energy marine environment, in shallower water than the facies with flat larger foraminifera (i.e. FA-2 and FA-3; Boudagher-Fadel *et al.*, 2000; Hallock & Pomar, 2008; Bou-Dagher-Fadel, 2018) and possibly above the fair-weather wave base (FWWB) due to the limited amount of matrix.

Vertical and lateral distribution of the facies associations

Facies Association 1 (aphotic zone; Table 2; Fig. 5) was only identified in the offshore well-cuttings from Pyrenees 1 and Macedon 1 (P1 and M1; Figs 3 and 14), and importantly, FA-1 is the only facies association identified in those wells, despite the fact that the wells include the full stratigraphic interval studied (i.e. interval between planktonic foraminiferal zones N5 and N7, equivalent to 21.81 to 16.4 Ma based on Blow, 1969, and Wade *et al.*, 2011; Figs 3 and 14). Facies Association 2 (base oligophotic zone; Figs 6 to 8) was identified at the base of the northerly onshore sections (BC and SC; Figs 2A and 14), in the basal part of the older outcrops investigated (i.e. respectively belonging to the Te Australasian 'Letter-stage' and to the lower part of a succession belonging to the N5-N7 Planktonic foraminifera N-zone; Table 1; Fig. 14). Facies Association 3 (oligophotic zone; Figs 9 to 11) was identified in the central and upper, younger parts of the Shothole Canyon and unnamed canyon north of Badjirrajirra Creek sections, directly overlying FA-2 (SC and BG; Fig. 2). FA-3 was also identified at the base of the centrally located Charles Knife Road
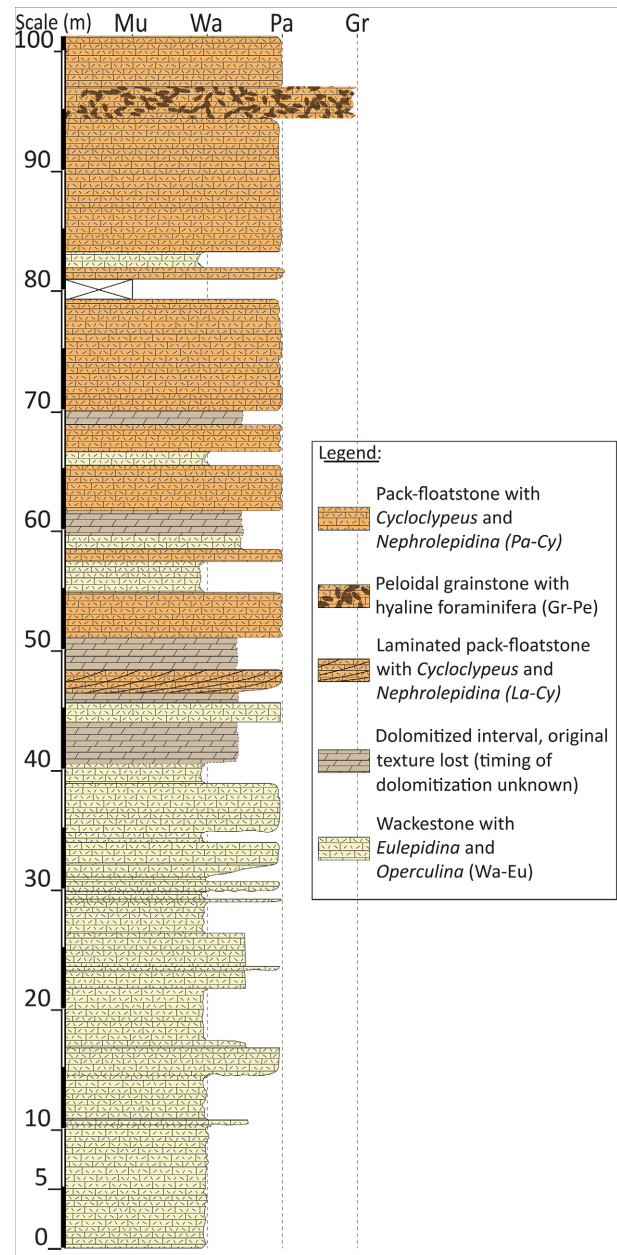
Fig. 11. Lithostratigraphic column of the upper Shothole Canyon section showing the vertical organization of facies in Facies Association 3 (FA-3). Note that the succession is shallowing upward, with more *Lepidocyclina (Eulepidina)* in its lower part (facies Wa-Eu) and more *Lepidocyclina (Nephrolepidina)* in its upper part (facies Pa-Cy and La-Cy).

section (CKR; Fig. 14). Facies Association 4 (mesophotic zone; Fig. 12) was identified in the upper part of the Charles Knife Road section overlying FA-3, and in the lower and central parts of the Mount Lefroy section (ML; Fig. 2). Then, FA-4 was only identified in relatively
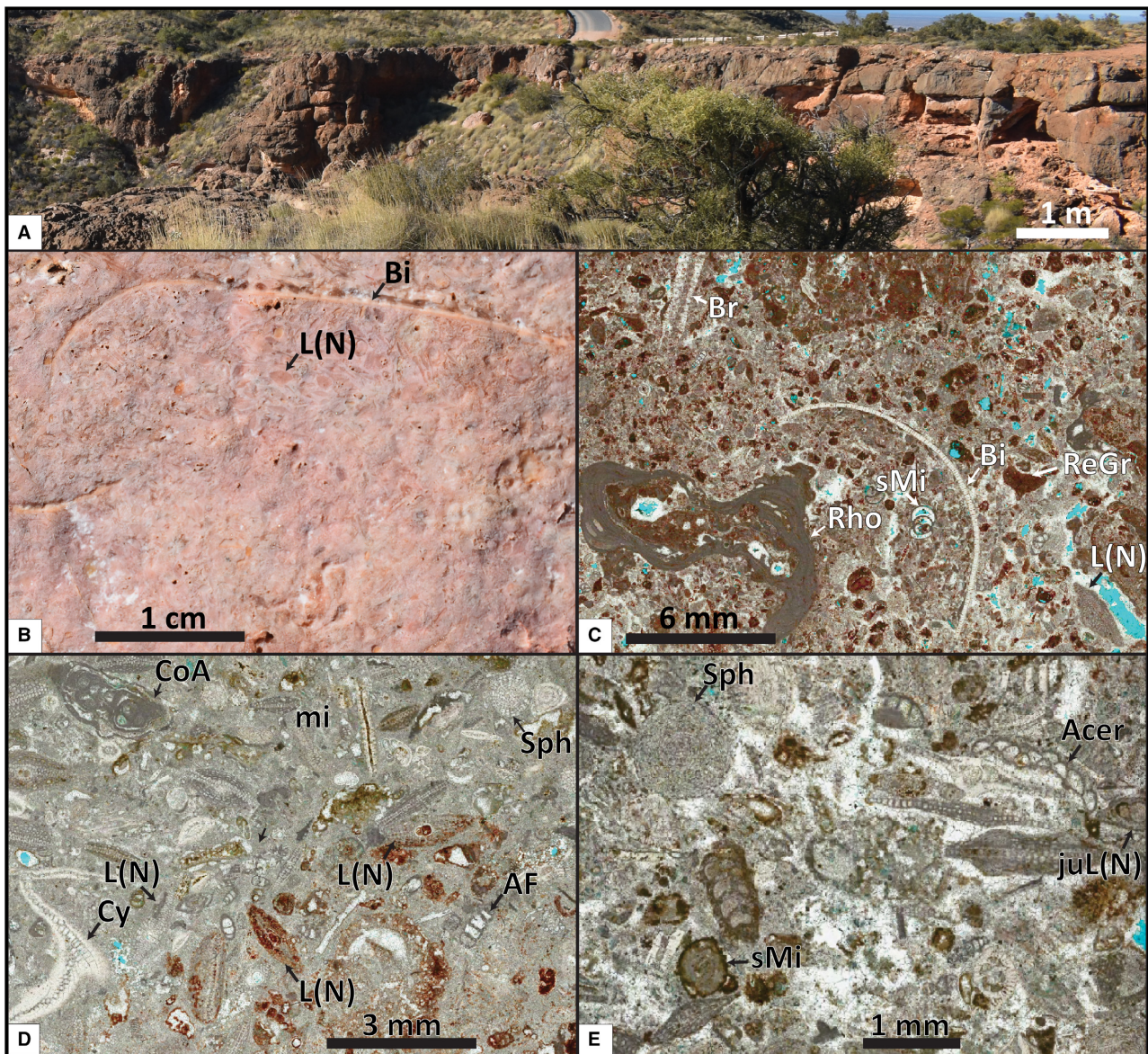
Fig. 12. Outcrop photograph and photomicrographs of the facies from Facies Association 4 (FA-4) along the Charles Knife Road. (A) Outcrop photograph of packstone–grainstone with *Lepidocyclina* (*Nephrolepidina*), *Cycloclypeus* and coralline algae (facies Gr-Ne, the only facies in FA-4). (B) Close-up outcrop view of the facies Gr-Ne, note the presence of robust forms of *Lepidocyclina* [*Nephrolepidina*) (L(N)] and of bivalve shell (Bi). (C) to (E) Photomicrographs of the facies Gr-Ne (plane-polarized light), illustrating the diversity of foraminiferal assemblages, which can change at the thin section scale; all images have in common the presence of thickened forms of *Lepidocylina* (*Nephrolepidina*) (L(N)) and of oxidized grains embedded in a non-oxidized micritic matrix; the samples used for the thin sections were collected 30 cm apart from one another, illustrating the high variability in this facies. Acer, Acervulina; AF, agglutinated foraminifera; Bi, bivalve; Br, bryozoan; CoA, coralline algae; Cy, *Cycloclypeus*; juL(N), juvenile Lepidocyclina; L(N), *Lepidocyclina (Nephrolepidina)*; mi, micrite; ReGr, relict grain; Rho, rhodolith; sMi, small miliolid; Sph, *Sphaerogypsina*.

young outcrops, belonging to the Lower Tf1 Australasian 'Letter-stage' and to the N7 planktonic foraminifera N-zone (Figs 4 and 14). Finally, Facies Association 5 (uppermost mesophotic zone; Fig. 13) was only identified in the upper part of the Mount Lefroy section, overlying FA-4 (Fig. 14). No strata from foraminiferal zones N5-N7 were identified in the onshore wells Exmouth 2 and Rough Range 1 (Ex2 and RR1; Table 1; Figs 2 and 14), whereas older

early Miocene deposits (i.e. belonging to the N3-N4 foraminiferal N-zone) and younger middle Miocene deposits (i.e. belonging to the N9 foraminiferal N-zone) are present (Table 1; Fig. 14).

DISCUSSION

Depositional model

This study indicates that the early Miocene strata exposed in the Cape Range Anticline accumulated on a broad carbonate platform prograding towards the north-west. Early Miocene facies indicate a shallower depositional environment towards the south-east (i.e. FA-5 and FA-4; Fig. 14) and a deeper depositional environment towards the north-west (i.e. FA-3 and FA-4; Fig. 14). All outcrops show shallowing-upward trends [i.e. FA-2 to FA-3 in Shothole Canyon (SC) and unnamed canyon north of Badjirrajirra Creek (BG); FA-3 to FA-4 in Charles Knife Road (CKR); FA-4 to FA-5 in Mount Lefroy (ML); Fig. 14]. The apparent light-related zonation of the facies suggests deposition in a mainly open setting, with shallower facies likely accumulated in an environment subject to the action of waves (for example, presence of robust large hyaline foraminifera with massive pillars and robust morphologies in FA-4 and FA-5) while deeper facies were likely accumulated in a calm environment only episodically affected by higher energy events (for example, presence of fragile giant and flat larger hyaline foraminifera in FA-2 and FA-3). This may reflect the absence of hydrodynamic barriers, which is further supported by the apparent absence of organic build-ups. These observations support deposition along a ramp profile prograding towards the north or the west.

Deposition along a ramp-profile is even more likely as the gradual changes in facies from the north-west to the south-east may reflect the transition from the outer ramp to the inner ramp. Indeed, sedimentary structures identified in FA-2 point towards a calm environment below the fair-weather wave base (FWWB) but with infrequent storm reworking (i.e. background accumulation of fine-grained facies interbedded with planar laminated or chaotic beds suggesting episodic higher energy events). Thus, FA-2 can be considered as accumulated in the outer-ramp (*sensu* Burchette & Wright, 1992; Fig. 15). Bioclasts and sedimentary structures from FA-3 also point towards accumulation in a calm environment, but in a shallower environment than FA-2, and possibly with more frequent higher

energy events (i.e. possibly current-induced facies, fine content lower than in FA-2). Hence, FA-3 could have accumulated in a mid-ramp setting (Fig. 15). Bioclasts in FA-4 indicate a higher-energy marine environment, while the presence of micrite suggests that FA-4 accumulated below the FWWB, in the mid-ramp. As micrite is scarcer in FA-5, this facies association may well have accumulated in an inner-ramp setting. No sedimentary structures were identified in FA-1, as this facies association was only identified from well cuttings. Since FA-1 is interpreted as having accumulated in a deeper environment than FA-2, FA-1 may have accumulated in the outer ramp or in the basin (Fig. 15). This is supported by the fine grain size, and by the relative abundance of planktonic foraminifera compared to other facies.

These observations collectively suggest that the early Miocene outcrops present in the Cape Range Anticline belong to the carbonate ramp that covered the NWS during the early Miocene (Fig. 1). Outcrops analyzed here may have accumulated on the outer ramp (i.e. FA-2) and mid-ramp (i.e. FA-3 and FA-4). The inner-ramp may have been identified from archived samples (FA-5) while the outer ramp was also identified from offshore well cuttings (FA-1). Seismic-well correlation (Riera, 2020) suggests that facies from Macedon 1 were accumulated landward of the distal break in slope, while facies from Pyrenees 1 were accumulated basinward of the distal break in slope (Fig. 3), in line with an accumulation in the outer ramp and slope. It may be noted that most of the inner-ramp has not been identified, and the absence of strata of N5-N7 age in the onshore wells Exmouth 2 and Rough Range 1 (Ex2 and RR1; Figs 2 and 14) suggests the presence of an intra-Miocene unconformity at the inferred location of the inner-ramp. Early Miocene limestones time-equivalent to the strata investigated in this study are present in the Giralia Anticline, and are interpreted as accumulated in a marginal lagoon *ca* 10 m deep (Haig *et al.*, 2020). The presence of a marginal lagoon does not contradict the ramp interpretation (cf. Burchette & Wright, 1992) and this lagoon may represent the shallowest part of the early Miocene ramp investigated here (Fig. 15).

The depositional model of this ramp contrasts with the well-known, distally steepened ramp from the western Mediterranean (Pomar, 2001b). The main difference in the overall setting of the two carbonate ramp systems appears to be the oceanographic setting, with the open oceanic
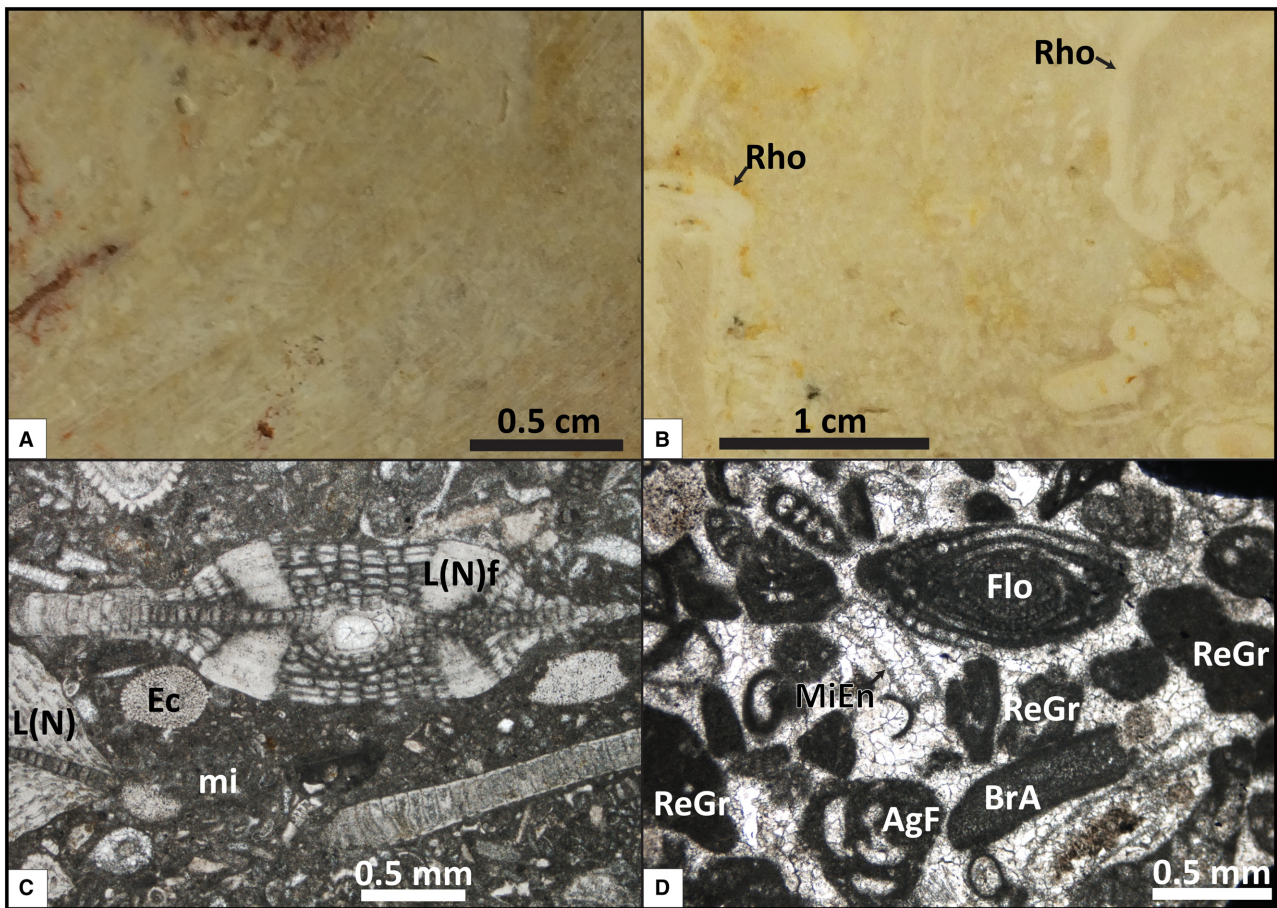
Fig. 13. Photographs and photomicrographs of samples collected in the Mount Lefroy area (Chaproniere, 1984b) characteristic of Facies Association 5 (FA-5). (A) and (B) Close-up views of the wackestone–grainstone with Miliolida and Rotaliida (facies Gr-Mi; Table 2) that locally contains abundant coralline algae (Rho) (A: sample UWA51907, B: sample UWA51908). (C) Photomicrograph of a thin section of the facies Gr-Mi (plane-polarized light), in an interval with micritic matrix (mi) and echinoderm debris (Ec), note the presence of massive pillars in *Lepidocyclina (Nephrolepidina) ferreroi* (L(N)f) and the robust morphology of the *Lepidocyclina (Nephrolepidina)* spp. (L(N)). (D) Photomicrograph of a thin section of the facies Gr-Mi (plane-polarized light), in an interval without micrite, highlighting the presence of *Flosculinella* (Flo), which have warm-water affinities, of agglutinated foraminifera (AgF), of branching algae (BrA) and of dissolved grains with a micrite envelope (MiEn).

margin conditions of the North West Shelf causing prevailing higher energy conditions. The inferred stronger impact of physical parameters as compared to biofacies in establishing platform architecture is not unusual, as reported for numerous other open oceanic carbonate platforms, such as the Marion Plateau (Northeast Australia; Isern *et al.*, 2005) and the Great Bahama Bank (Eberli & Ginsburg, 1987; Anselmetti *et al.*, 2000).

Heterozoan or photozoan?

Correlation of well and field data on pre-existing seismic interpretations (Young, 2001; Cathro *et al.*, 2003; Riera, 2020; Fig. 3) suggests that a

significant part of the ramp visible on seismic data (Figs 1 and 3) was formed in the aphotic zone (FA-1; Fig. 15), in an area where almost no coarse grains were produced/preserved, or reworked (i.e. facies association FA-1). The classification of this carbonate system as heterozoan or photozoan (*sensu* James, 1997) is therefore not straightforward, because it relies largely on the origin of the micropackstone matrix, which is a dominant component of the deeper facies (i.e. facies from FA-1, FA-2 and FA-3; Table 2). This micropackstone matrix has at least two possible origins: (i) allogenic sedimentation, with the micropackstones being made of debris of photozoan organisms, such as larger
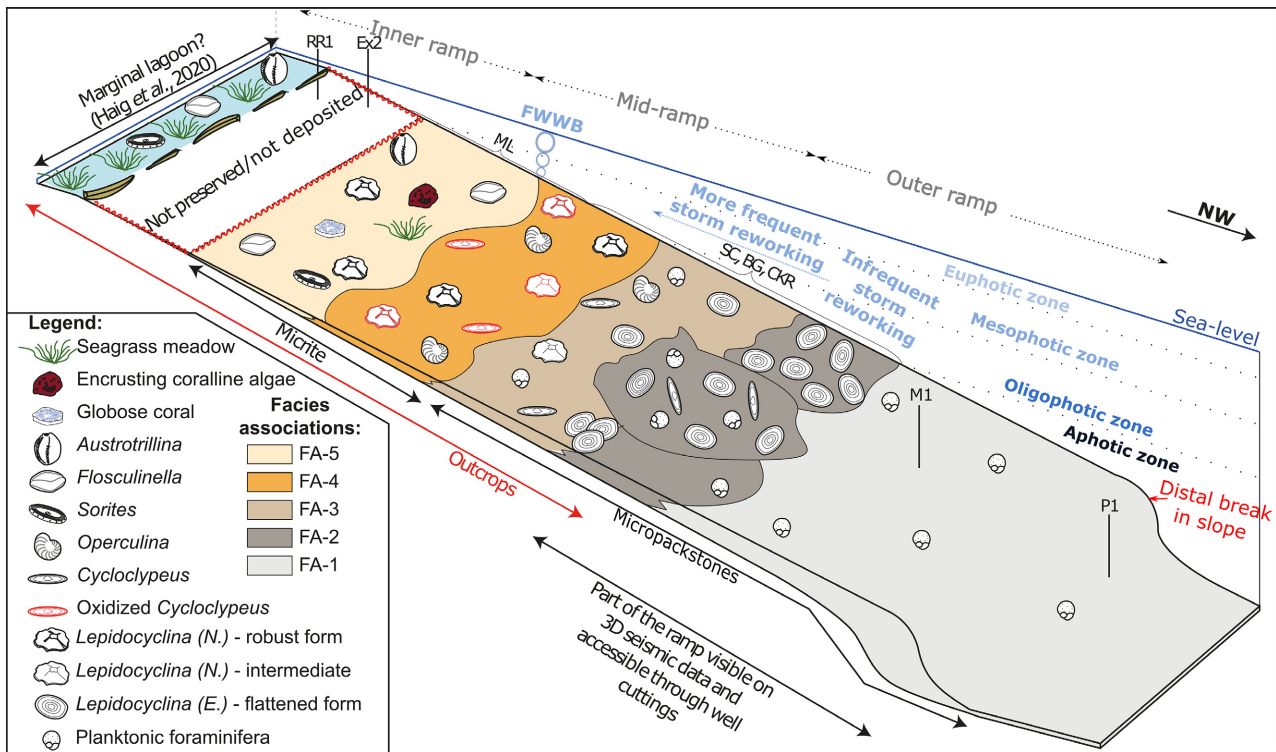
Fig. 14. Vertical and lateral distribution of the facies associations, with the more distal facies located in the north-west of the study area, dominantly offshore, and with the more proximal facies located in the south-east of the study area, exclusively onshore. The location of the different sections is indicated in Fig. 2A. RR1, onshore well Rough Range South No. 1; Ex2, onshore well Exmouth No. 2; ML, Mount Lefroy; CKR, Charles Knife Road; BG, unnamed canyon north of Badjirrajirra Creek; SC, Shothole Canyon; M1, offshore well Macedon 1; P1, offshore well Pyrenees 1. NW, north-west. All depths are in metres (mbs, metres below surface; mRT, metres below rotary table; m, metres above base of outcrop).

foraminifera, and then reworked into the aphotic zone; or (ii) *in situ* production by infaunal and pelagic organisms. Larger benthic foraminifera are among the main carbonate producers in modern tropical environments (Hohenegger, 2006; Renema, 2018). Micropackstones composed of debris of larger foraminifera and other shallower bioclasts produced in the photic zone, and then reworked in the aphotic zone by wave and marine currents, is indeed possible for the facies described here. Equally feasible, the micropackstone matrix could also result from, or have an element of, *in situ* biogenic production based on high production of carbonate sediment by heterotrophic benthic organisms, and/or by pelagic rain, in both cases followed by taphonomic degradation subsequent to sediment accumulation (e.g. Cherns & Wright, 2000, 2009). Better constraining the mode of formation of the micropackstones is thus crucial to better understand the processes driving carbonate production along the early Miocene ramps of the southern NWS and other comparable systems

globally. The overall lack of identifiable carbonate grains in the micropackstones prevents the classification of this ramp as a heterozoan or photozoan system. The shallower part of the ramp, however, developed in the photic zone, with its abundant and diverse larger benthic foraminifera that are light reliant, warm-water biota, and therefore photozoan in origin (Wilson & Vecsei, 2005).

Palaeoenvironmental implications

Water temperature

The scarcity of corals and the apparent absence of reefal build-ups along the early Miocene ramp of the southern North West Shelf, together with its previous classification as a heterozoan system, have been used to infer that the climate was too cold for coral proliferation during the deposition of the ramp (Collins *et al.*, 2006). However, no studies have specifically focused on the ocean water temperature along the NWS during the early Miocene, and a cool–temperate

Fig. 15. Depositional model illustrating the three-dimensional distribution of facies associations along the early Miocene ramp investigated (i.e. planktonic foraminiferal zones N5-N7, equivalent 21.81 to 16.40 Ma). The subdivision of the photic zone is based on the terminology from Pomar (2001a) which partially builds on the presence of selected genera of larger benthic foraminifera (Hottinger, 1997; Beavington-Penney & Racey, 2004). The subdivision of the ramp into inner ramp, mid-ramp and outer ramp follows Burchette & Wright (1992). FWWB, fair-weather wave base; RR1, onshore well Rough Range South No. 1; Ex2, onshore well Exmouth No. 2; ML, Mount Lefroy; SC, Shothole Canyon; BG, unnamed canyon north of Badjirrajirra Creek; CKR, Charles Knife Road; M1, offshore well Macedon 1; P1, offshore well Pyrenees 1. The location of the different sections is indicative, for exact location see Fig. 2A.

to sub-tropical climate was dominantly inferred based on the seismic ramp morphology. Ambiguity regarding the temperature of the seawater of the NWS during the early Miocene has already been reported by Rosleff-Soerensen *et al.* (2012), who noted that there are tropical species of planktonic foraminifera in the ramp system of the Browse Basin (for example, *Globorotalia kugleri*, *Globigerina* cf. *venezuelana*, *Globorotalia peripheroronda* and *Globigerinoides trilobus*). Additionally, studies of offshore seismic surveys indicate that reefs may have been locally present in the northernmost part of the NWS since the late Burdigalian (i.e. foraminiferal zone N6; Gorter *et al.*, 2002; Saqab & Bourget, 2016; Belde *et al.*, 2017). McCaffrey *et al.* (2020) noted that there were species of larger foraminifera with warm-water affinities in the Cape Range area during the late Oligocene, whereas, in contrast, the overall Oligo–Miocene

outcrops were described as having accumulated in an environment too cool for prolific coral reef production by Collins *et al.* (2006). Haig *et al.* (2020) reported the presence of late Burdigalian (i.e. 19 to 16 Ma) sediment-dwelling alveolinids (i.e. *Flosculinella*) in the marginal lagoon bordering the carbonate ramp investigated in this study, with the southernmost Burdigalian *Flosculinella* identified in the vicinity of the modern Lake MacLeod, 160 km south of the area investigated here. This supports a warm oceanographic setting during the late Burdigalian, and suggests minimum winter temperatures above 17°C based on comparison with modern Western Australian alveolinids (Logan & Cebulski, 1970).

Most extant larger benthic foraminifera live in warm marine waters, mainly in reefs and in the shallow part of carbonate shelves (Langer & Hottinger, 2000; BouDagher-Fadel, 2018). The abundance of larger foraminifera in the early Miocene

facies described in this study suggest that sedimentation was taking place in warm waters. In particular, the presence of *Cycloclypeus* in the distal part of the ramp, and of *Flosculinella* in the more proximal part, support this interpretation. Indeed, modern *Cycloclypeus carpenteri* live in areas with high sea-surface temperatures in the central Indo-Pacific, and the distribution of *Cycloclypeus carpenteri* overlaps the centres of diversity for corals and mangroves (Langer & Hottinger, 2000). *Cycloclypeus carpenteri* is, for example, present in the Great Barrier Reef (Langer & Hottinger, 2000). Moreover, even though the alveolinid *Flosculinella* is extinct, modern alveolinids such as *Borelis sp.* and *Alveolinella quoyii* live in waters between 22°C and 34°C (Langer & Hottinger, 2000), and *Borelis* is typically associated with tropical rimmed platforms (e.g. Betzler, 1997). Amphisteginids and soritids have a larger living range and can occur in warm temperate areas (Betzler *et al.*, 1997), although they are more abundant in the tropics (Langer & Hottinger, 2000). In general, modern larger benthic foraminifera live in tropical to warm temperate waters with a 15 to 20°C winter minimum isotherm (Langer & Hottinger, 2000; Renema, 2018). Soritids, alveoliniids, *Amphistegina* and *Cycloclypeus*, which are all present in the early Miocene ramp described here, are now abundant in the central Indo-Pacific realm, from Hawaii (eastern extension) to the Maldives (westward extension; Langer & Hottinger, 2000). The early Miocene assemblages of larger foraminifera described here are similar to the early Miocene foraminiferal assemblages from Asia, as *Flosculinella*, *Austrotrillina*, *Amphistegina*, *Lepidocyclina (Eulepidina)*, *Lepidocyclina (Nephrolepidina)*, including the species *L. (N.) ferreroi*, *Miogypsinoides*, *Operculina* and *Cycloclypeus* were all present in the tropical waters of south-east Asia during the early Miocene (Allan *et al.*, 2000; Boudagher-Fadel & Lord, 2000; Boudagher-Fadel & Lokier, 2005; Renema, 2007).

The overall scarcity of corals and green algae in the outcrops and samples studied here does not in itself conflict with the interpretation of an accumulation in warm waters. Indeed, corals and green algae are locally scarce in the Miocene equatorial platforms of south-east Asia, and Miocene carbonate facies composed of larger benthic foraminifera, coralline algae and rare *Halimeda* have been reported in those low latitude, warm-water carbonate platforms (Wilson & Vecsei, 2005). In the equatorial platforms of south-east Asia, the development of corals was locally hindered by unfavourable conditions, including high terrestrial runoff, nutrient upwelling, strong currents, high subsidence rates and/or lack of stable substrate (Wilson & Lokier, 2002; Wilson & Vecsei, 2005). Similarly, coral reef development in the inner part of the ramp investigated here could have been hampered by a range of local or regional palaeo-oceanographic and environmental conditions. Even an early taphonomic effect might be considered, given the very limited traces of aragonitic skeletal material (e.g. Cherns & Wright, 2000, 2009). Thus, in view of the considerations above, it is inferred that during the early Miocene, the oceanic waters of the NWS were warm, despite the shelf being located on a western continental margin, and despite the absence of observation of organic build-ups.

At present, the oceanic waters of the NWS are warmed by the south flowing Leeuwin current, and a proto-Leeuwin current may have already been active during the Miocene, based on the observation of Miocene taxa with warm-water affinities in southern Australia (McGowran *et al.*, 1997). Field investigations in southern Australia indicate that this Miocene southward flow was at its highest during the middle Miocene (McGowran *et al.*, 1997) or late early to early middle Miocene (O'Connell *et al.*, 2012). The existence of a strong middle Miocene Leeuwin-current style oceanic circulation is also supported by the presence of diverse middle Miocene corals in the Cape Range Anticline (Riera *et al.*, 2021). In addition, studies of seismic data show a lower Miocene ramp to middle Miocene rimmed platform transition along the NWS (e.g. Rosleff-Soerensen *et al.*, 2012; McCaffrey *et al.*, 2020), and also reveal the possible existence of a middle Miocene(?) 'Little Barrier Reef' in the Bight Basin (southern margin of Australia; Feary & James, 1995). The early Miocene waters of the NWS – in which the ramp investigated here developed – may have been similarly warmed by a tropical south-flowing current. This supports a Miocene or older origin of the proto-Leeuwin current, that has already been proposed by several studies (e.g. Feary & James, 1995; McGowran *et al.*, 1997; Wyrwoll *et al.*, 2009; O'Connell *et al.*, 2012). It is however also possible that the early Miocene warm marine environment simply reflects the overall warm climate of the early Miocene (see Mudelsee *et al.*, 2014).

Nutrient levels

Most extant larger benthic foraminifera live in waters poor in nutrients (Langer & Hottinger,

2000; BouDagher-Fadel, 2018), although they can also live in regions with coastal siliciclastic influx and turbidity (Novak & Renema, 2018). In the ramp studied here, the presence of giant and flat *Lepidocyclina (Eulepidina) badjirraensis* and of flat *Cycloclypeus* could indicate that the oligophotic zone was in calm and deep waters. In this zone the waters would have been oligotrophic during the formation of the ramp – at least periodically – because flat Rotaliida only live at great water depths, and cannot thrive in the absence of a deep-water oligophotic zone (Hallock, 1987).

Collins *et al.* (2006) reported periodic influx of terrigenous clays in the early Miocene succession in the Shothole Canyon area (Fig. 2A). This suggests that the water column was not permanently oligotrophic, and that water quality may have fluctuated. This may explain why larger foraminifera – with a relatively short generation span ranging from a couple of months to a couple of years (Krüger *et al.*, 1997; Renema & Troelstra, 2001) – may have been promoted over coral reefs, which require much longer time-scales – centennial to millennial – to fully re-establish after destruction (Webster *et al.*, 2018).

Along the modern Western Australian margin, proximal shallow-water carbonate production is low overall, possibly because of fluctuations in water quality caused by saline downwelling coming from marginal lagoons, such as Shark Bay, or by influx of siliciclastic sediments (Dix, 1989; Dix *et al.*, 2005). These processes are likely to be impacting carbonate production in the inner-ramp, enabling only limited proximal carbonate production dominated by seagrass meadows, larger foraminifera (for example, *Amphisorus*, *Amphistegina* and *Heterostegina*), mollusc and coralline algae (James *et al.*, 1999; Collins *et al.*, 2014). Comparable processes may have been active in the southern NWS during the early Miocene, as suggested by periodic influx of terrigenous clays in FA-2 (see also Collins *et al.*, 2006), and by the presence of fine angular quartz grains in the marly micropackstones from FA-1. In addition, it is suggested that the extensive normal marine to metahaline marginal lagoon east of the ramp during the late Burdigalian (19 to 16 Ma; Haig *et al.*, 2020) may be considered a plausible source of saline downwelling. As a consequence, it is proposed that the quality of water in the innermost part of the ramp may have periodically deteriorated, possibly over biennial to decennial timescales, as the larger species of foraminifera, such as *Lepidocyclina (Eulepidina) badjirraensis*,

need stable oligotrophic conditions not affected by seasonal variations to proliferate (Renema & Troelstra, 2001).

Offshore currents

A noteworthy, somewhat puzzling aspect of the sediment composition across this ramp is that the more proximal facies (i.e. facies from FA-4 and FA-5) are characterized by a micrite matrix and no quartz grains, whereas all deeper facies are characterized by a matrix made of bioclastic debris and varying amounts of fine angular quartz grains (i.e. facies from FA-1, FA-2 and FA-3). This may reflect the presence of an offshore current in the oligophotic zone that did not reach the mesophotic zone. Indeed, along the modern NWS, the Leeuwin current influences water movement in the upper *ca* 300 m of the water column (James *et al.*, 2004), creating a particularly strong shear on the outer shelf (Collins *et al.*, 2014). Similarly, during the early Miocene, sedimentation along the outer ramp and distal break in slope may have been influenced by the proto-Leeuwin current, that may have been capable of shaping platform morphology and episodically carrying fine angular quartz grains discharged by rivers from the Pilbara coast into the oligophotic zone of this platform. The potential impact of ocean currents on carbonate platform geometries has been demonstrated elsewhere (e.g. Anselmetti *et al.*, 2000; Isern *et al.*, 2005; Eberli *et al.*, 2010; Betzler *et al.*, 2016a,b, 2014; Lüdmann *et al.*, 2016, 2018). Moreover, the 'marly micropackstones' described in this study have similarities with the 'fine grained bioclastic packstones' described by Lüdmann *et al.*, 2018, p.18) in a carbonate delta drift (i.e. formed under a current-dominated depositional regime), and similarly, the grains in the 'marly micropackstones' could have experienced substantial current transport before accumulation. The presence of flat larger foraminifera in Facies Associations 2 and 3 [i.e. *Cycloclypeus* and *Lepidocyclina (E.) badjirraensis*] indicates that the marine environment was calm when these organisms where thriving, suggesting that this potential offshore current system was only occasionally interacting with the seafloor. It should however be noted that the decrease in quartz content in shallower facies may also be an observational bias, with the outcropping mesophotic facies being slightly younger than the outcropping oligophotic ones (Table 1; Fig. 14). Indeed, quartz content within the late

Pleistocene to Holocene sediment of the NWS seems to be controlled by the climate of the coast bordering the NWS, with more quartz grains and less micrite present in sediments accumulated during wetter intervals (Hallenberger *et al.*, 2019). Similarly, the decrease in quartz content and increase in micrite in shallower, younger facies possibly indicate continental aridification towards the end of the early Miocene (Fig. 14).

CONCLUSION

The results of this sedimentological study integrating descriptions of field exposures, archived onshore samples and offshore well cuttings are used to propose a depositional model for the extensive carbonate ramp that developed on the North West Shelf (NWS) during the early Miocene. Facies partitioning along the ramp profile was primarily controlled by light, with: (i) micritic foraminiferal wackestone–grainstones with robust *Lepidocyclina*, *Austrotrillina*, *Flosculinella*, *Sorites*, green algae and coralline algae accumulated in the inferred mesophotic zone; (ii) marly micropackstones with locally abundant flat *Lepidocyclina*, *Cycloclypeus* and *Operculina* in the inferred oligophotic zone; and (iii) barren marly micropackstones in the inferred aphotic zone. Despite the absence of field evidence for diverse coral assemblages or seismic evidence for reefal build-ups, the assemblages of larger foraminifera suggest that the ramp developed in warm waters.

ACKNOWLEDGMENTS

DATA AVAILABILITY STATEMENT

Thin sections from offshore well cuttings are archived at the Department of Mines, Industry Regulation and Safety, Western Australia. Field samples and thin sections from field samples are archived at the Edward de Courcy Clarke Earth Science Museum, University of Western Australia (UWA180000–UWA180418).

REFERENCES

Allan, T.L., **Trotter, J.A.**, **Whitford, D.J.** and **Korsch, M.J.** (2000) Strontium isotope stratigraphy and the Oligocene-Miocene T-Letter "Stages" in Papua New Guinea. In: *Papua New Guinea's Petroleum Industry in the 21st Century: Proceedings of the Fouth PNG Petroleum Convention, 29th-31st May, 2000* (Eds Buchanan, P.G., Grainge, A.M. and Thomton, R.C.N.), pp. 155–168. PNG Chamber of Mines and Petroleum, Port Moresby.

Allen, A.D. (1993) Outline of the geology and hydrogeology of Cape Range, Carnarvon Basin, Western Australia. In: *The Biogeography of Cape Range, Western Australia.* Records of the Western Australian Museum Supplement No. 45 (Ed. Humphreys, W.F.), pp. 25–38. Western Australian Museum, Perth Western Australia.

Anell, I. and **Wallace, M.W.** (2019) A fine balance: Accommodation dominated control of contemporaneous cool-carbonate shelf-edge clinoforms and tropical reef-margin trajectories, North Carnarvon Basin, Northwestern Australia. *Sedimentology*, **67**, 96–117.

Anselmetti, F.S., **Eberli, G.P.** and **Ding, Z.D.** (2000) From the Great Bahama Bank into the straits of Florida: A margin architecture controlled by sea-level fluctuations and ocean current. *Bull. Geol. Soc. Am.*, **112**, 829–844.

Apthorpe, M. (1988) Cainozoic depositional history of the North West Shelf. In: *The North West Shelf, Australia* (Eds Purcell, P.G. and Purcell, R.R.), pp. 55–84. Proceedings of the Petroleum Exploration Society of Australia Symposium, Perth, WA.

Beavington-Penney, S.J. and **Racey, A.** (2004) Ecology of extant nummulitids and other larger benthic foraminifera: Applications in palaeoenvironmental analysis. *Earth-Science Rev.*, **67**, 219–265.

Beavington-Penney, S.J., **Wright, V.P.** and **Racey, A.** (2005) Sediment production and dispersal on foraminifera-dominated early Tertiary ramps: The Eocene El Garia Formation, Tunisia. *Sedimentology*, **52**, 537–569.

Belde, J., **Back, S.**, **Bourget, J.** and **Reuning, L.** (2017) Oligocene and miocene carbonate platform development in the browse basin, Australian Northwest Shelf. *J. Sediment. Res.*, **87**, 795–816.

Betzler, C. (1997) Ecological Controls on Geometries of Carbonate Platforms: Miocene/Pliocene Shallow-water Microfaunas and Carbonate Biofacies from the Queensland Plateau (NE Australia). *Facies*, **37**, 147–166.

Betzler, C., **Brachert, T.C.** and **Nebelsick, J.** (1997) The warm temperate carbonate province a review of the facies, zonations, and delimitations. *CFS Cour. Forschungsinstitut Senckenb.*, **201**, 83–99.

Betzler, C., **Eberli, G.P.**, **Kroon, D.**, **Wright, J.D.**, **Swart, P.K.**, **Nath, B.N.**, **Alvarez-Zarikian, C.A.**, **Alonso-Garciá, M.**, **Bialik, O.M.**, **Blättler, C.L.**, **Guo, J.A.**, **Haffen, S.**, **Horozal, S.**, **Inoue, M.**, **Jovane, L.**, **Lanci, L.**, **Laya, J.C.**, **Mee, A.L.H.**, **Lüdmann, T.**, **Nakakuni, M.**, **Niino, K.**, **Petruny, L.M.**, **Pratiwi, S.D.**, **Reijmer, J.J.G.**, **Reolid, J.**, **Slagle, A.L.**, **Sloss, C.R.**, **Su, X.**, **Yao, Z.** and **Young, J.R.** (2016a) The abrupt onset of the modern South Asian Monsoon winds. *Sci. Rep.*, **6**, 1–10.

Betzler, C., **Hübscher, C.**, **Lindhorst, S.**, **Lüdmann, T.**, **Reijmer, J.J.G.** and **Braga, J.-C.** (2016b) Lowstand wedges in carbonate platform slopes (Quaternary, Maldives, Indian Ocean). *Depos. Rec.*, **2**, 196–207.

Betzler, C., **Lindhorst, S.**, **Eberli, G.P.**, **Lüdmann, T.**, **Möbius, J.**, **Ludwig, J.**, **Schutter, I.**, **Wunsch, M.**, **Reijmer, J.J.G.** and **Hübscher, C.** (2014) Periplatform drift: The combined result of contour current and off-bank transport along carbonate platforms. *Geology*, **42**, 871–874.

Blow, W.H. (1969) Late Middle Eocene to Recent Planktonic Foraminiferal Biostratigraphy. *Proc. First Int. Conf. Planktonic Microfossils*, Geneva 1967, **1**, 199–422.

Bosence, D. (2005) A genetic classification of carbonate platforms based on their basinal and tectonic settings in the Cenozoic. *Sediment. Geol.*, **175**, 49–72.

BouDagher-Fadel, M.K. (2018) *Evolution and Geological Significance of Larger Benthic Foraminifera*, 2nd edn. UCL PRESS, London, UK, 693 pp.

Boudagher-Fadel, M.K. and **Lokier, S.W.** (2005) Significant Miocene larger foraminifera from South Central Java. *Rev. Paleobiol.*, **24**, 291–309.

Boudagher-Fadel, M.K., **Lord, A.R.** and **Banner, F.T.** (2000) Some Miogypsinidae (foraminifera) in the Miocene of Borneo and nearby countries. *Rev. Paleobiol.*, **19**, 137–156.

Boudagher-Fadel, M. and **Lord, A.** (2000) The evolution of Lepidocyclina (L.) Isolepidinoides, L. (Nephrolepidina) Nephrolepidinoides sp nov., L. (N.) Brouweri and L. (N.) Ferreroi in the late Oligocene-Miocene of the Far East. *J. Foraminifer. Res.*, **1**, 71–76.

Bradshaw, M.T., **Yeates, A.N.**, **Beynon, R.M.**, **Brakel, A.T.**, **Langford, R.P.**, **Totterdell, J.M.** and **Yeung, M.** (1988) Palaeogeographic evolution of the North West Shelf Region. In: *The North West Shelf, Australia* (Eds Purcell, P.G. and Purcell, R.R.), pp. 29–54. Proceedings of the Petroleum Exploration Society of Australia Symposium, Perth, WA.

Braga, J.C., **Bassi, D.** and **Piller, W.E.** (2010) Palaeoenvironmental significance of Oligocene-Miocene coralline red algae – a review. In: *Carbonate Systems During the Oligocene-Miocene Climatic Transition* (Eds Mutti, M., Piller, W. and Betzler, C.), *IAS Special Publication*, **42**, 165–182.

Brandano, M., **Cornacchia, I.**, **Tomassetti, L.**, **Roma, S.** and **Moro, P.A.** (2017) Global versus regional influence on the carbonate factories of Oligo-Miocene carbonate platforms in the Mediterranean area. *Mar. Pet. Geol.*, **87**, 188–202.

van Buchem, F.S.P., **Allan, T.L.**, **Laursen, G.V.**, **Lotfpour, M.**, **Moallemi, A.**, **Monibi, S.**, **Motiei, H.**, **Pickard, N.A.H.**, **Tahmasbi, A.R.**, **Vedrenne, V.** and **Vincent, B.** (2010) Regional stratigraphic architecture and reservoir types of the Oligo-Miocene deposits in the Dezful Embayment (Asmari and Pabdeh Formations) SW Iran. *Geol. Soc. Spec. Publ.*, **329**, 219–263.

Burchette, T.P. and **Wright, V.P.** (1992) Carbonate ramp depositional systems. *Sediment. Geol.*, **79**, 3–57.

Cathro, D.L., **Austin, J.A.J.** and **Moss, G.D.** (2003) Progradation along a deeply submerged Oligocene-Miocene heterozoan carbonate shelf: How sensitive are clinoforms to sea level variations? *Am. Assoc. Pet. Geol. Bull.*, **87**, 1547–1574.

Cathro, D.L. and **Karner, G.D.** (2006) Cretaceous-Tertiary inversion history of the Dampier Sub-basin, northwest Australia: Insights from quantitative basin modelling. *Mar. Pet. Geol.*, **23**, 503–526.

Chaproniere, G.C.H. (1975) Palaeoecology of Oligo-Miocene larger Foraminiferida, Australia. *Alcheringa An Australas. J. Palaeontol.*, **1**, 37–58.

Chaproniere, G.C.H. (1977) *Studies on Foraminifera from Oligo-Miocene Sediments, North-West Western Australia.* PhD Thesis. University of Western Australia, Perth, WA, 486 pp.

Chaproniere, G.C.H. (1984a) *Oligocene and Miocene larger Foraminiferida from Australia and New Zealand.* Australian Government Publishing Service, Canberra, ACT, 74 pp.

Chaproniere, G.C.H. (1984b) The Neogene Larger Foraminiferal Classification. *Palaeogeogr. Palaeoclimatol. Palaeoecol.*, **46**, 25–35.

Cherns, L. and **Wright, V.P.** (2000) Missing molluscs as evidence of large-scale, early skeletal aragonite dissolution in a Silurian sea. *Geology*, **28**, 791–794.

Cherns, L. and **Wright, V.P.** (2009) Quantifying the impacts of early diagenetic aragonite dissolution on the fossil record. *Palaios*, **24**, 756–771.

Christensen, B.A., **Renema, W.**, **Henderiks, J.**, **De Vleeschouwer, D.**, **Groeneveld, J.**, **Castañeda, I.S.**, **Reuning, L.**, **Bogus, K.**, **Auer, G.**, **Ishiwa, T.**, **McHugh, C.M.**, **Gallagher, S.J.** and **Fulthorpe, C.S.** (2017) Indonesian Throughflow drove Australian climate from humid Pliocene to arid Pleistocene. *Geophys. Res. Lett.*, **44**, 6914–6925.

Cohen, K.M., **Finney, S.C.**, **Gibbard, P.L.** and **Fan, J.-X.** (2013) The ICS international chronostratigraphic chart. *Episodes*, **36**(3), 199–204.

Collins, L.B. (2002) Tertiary Foundations and Quaternary Evolution of Coral reef Systems of Australia's North West Shelf. In: *The Sedimentary Basins of Western Australia 3: Proceedings of Petroleum Exploration Society of Australia Symposium* (Eds Keep, M. and Moss, S.J.), pp. 129–152. Petroleum Exploration Society of Australia, Perth, WA.

Collins, L.B., **James, N.P.** and **Bone, Y.** (2014) Carbonate shelf sediments of the western continental margin of Australia. In: *Continental Shelves of the World: Their Evolution During the Last Glacio-Eustatic Cycle* (Eds Chiocci, F.L. and Chivas, A.R.), *Geological Society, London, Memoirs*, **41**, 255–272.

Collins, L.B., **Read, J.F.**, **Hogarth, J.W.** and **Coffey, B.P.** (2006) Facies, outcrop gamma ray and C-O isotopic signature of exposed Miocene subtropical continental shelf carbonates, North West Cape, Western Australia. *Sediment. Geol.*, **185**, 1–19.

Condon, M.A., **Johnstone, D.** and **Perry, W.J.** (1955) The Cape Range Structure Western Australia, part 1. In: *Bulletin 21*, 2nd edn. pp. 7–48. Bureau of Mineral Ressources, Geology and Geophysics of the Commonwealth of Australia, Canberra, ACT.

Conesa, G.A.R., **Favre, E.**, **Münch, P.**, **Dalmasso, H.** and **Chaix, C.** (2005) Biosedimentary and Paleoenvironmental Evolution of the Southern Marion Platform from the Middle to Late Miocene (Northeast Australia, ODP Leg 194, Sites 1196 and 1199). In: *Proceedings of the Ocean Drilling Program, Scientific Results*, Vol. **194** (Eds Anselmetti, C., Isern, F.S., Blum, A.R. and Betzler, P.), *Ocean Drilling Program*, **194**, 38.

Crespin, I. (1944) The occurence of the genus *Conoclypus* in the North-West Division, Western Australia. *J. R. Soc. West. Aust.*, **28**, 75–77.

Crespin, I. (1955) The Cape Range Structure, Western Australia, part 2. In: *Bulletin 21*, 2nd edn, pp. 49–81. Bureau of Mineral Ressources, Geology and Geophysics of the Commonwealth of Australia, Canberra, ACT.

De Deckker, P., **Barrows, T.T.** and **Rogers, J.** (2014) Land-sea correlations in the Australian region: Post-glacial onset of the monsoon in northwestern Western Australia. *Quat. Sci. Rev.*, **105**, 181–194.

Dix, G.R. (1989) High-energy, inner shelf carbonate facies along a tide-dominated non-rimmed margin, northwestern Australia. *Mar. Geol.*, **89**, 347–362.

Dix, G.R., **James, N.P.**, **Kyser, T.K.**, **Bone, Y.** and **Collins, L.B.** (2005) Genesis and Dispersal of Carbonate Mud Relative to Late Quaternary Sea-Level Change Along a Distally-Steepened Carbonate Ramp (Northwestern Shelf, Western Australia). *J. Sediment. Res.*, **75**, 665–678.

Dunham, R.J. (1962) Classification to the carbonate rocks according to depositional texture. In: *Classification of Carbonate Rocks* (Ed. Ham, W.E.), pp. 108–121. AAPG, Tulsa, OK.

Eberli, G.P., **Anselmetti, F.S.**, **Isern, A.R.** and **Delius, H.** (2010) Timing of changes in sea-level and currents along Miocene platforms on the Marion Plateau, Australia. *Cenozoic Carbonate Syst. Australas.*, **95**, 219–242.

Eberli, G.P. and **Ginsburg, R.N.** (1987) Segmentation and coalescence of Cenozoic carbonate platforms, northwestern Great Bahama Bank. *Geology*, **15**, 75–79.

Feary, D.A. and **James, N.P.** (1995) Cenozoic biogenic mounds and buried Miocene(?) barrier reef on a predominantly cool-water carbonate continental margin - Eucla Basin, western Great Australian Bight. *Geology*, **23**, 427–430.

Flower, B.P. and **Kennett, J.P.** (1993) Middle Miocene ocean–climate transition: High-resolution oxygen and carbon isotopic records from Deep Sea Drilling Project Site 588A, Southwest Pacific. *Paleoceanography*, **8**, 811–843.

Gallagher, S.J., **Wallace, M.W.**, **Hoiles, P.W.** and **Southwood, J.M.** (2014) Seismic and stratigraphic evidence for reef expansion and onset of aridity on the Northwest Shelf of Australia during the Pleistocene. *Mar. Pet. Geol.*, **57**, 470–481.

Gorter, J.D., **Rexilius, J.P.**, **Powell, S.L.** and **Bayford, S.W.** (2002) Late Early to Mid Miocene patch reefs, Ashmore Platform, Timor Sea - Evidence from 2D and 3D seismic surveys and petroleum exploration wells. *Sediment. Basins West. Aust. Proc. Pet. Explor. Soc. Aust. Symp.*, **3**, 355–375.

van de Graaff, W.J.E., **Denman, P.D.** and **Hocking, R.M.** (1976) Emerged Pleistocene marine terraces on Cape Range, Western Australia. Geological Survey of Western Australia, Annual Report for 1975, 62–70.

van de Graaff, W.J.E., **Denman, P.D.**, **Hocking, R.M.** and **Baxter, J.L.** (1980) *Yanrey-Ningaloo, Western Australia*. 1:250 000 Geological Series - Explanatory notes. SF49-12. Geological Survey of Western Australia, Perth, Western Australia, 24 pp.

Gradstein, F., **Ogg, J.** and **Smith, A.** (2005) *A Geologic Time Scale 2004*. Cambridge University Press, Cambridge, 589 pp.

Groeneveld, J., **Henderiks, J.**, **Renema, W.**, **McHugh, C.M.**, **De Vleeschouwer, D.**, **Christensen, B.A.**, **Fulthorpe, C.S.**, **Reuning, L.**, **Gallagher, S.J.**, **Bogus, K.**, **Auer, G.** and **Ishiwa, T.** (2017) Australian shelf sediments reveal shifts in Miocene Southern Hemisphere westerlies. *Sci. Adv.*, **3**, 1–8.

Haig, D.W., **Smith, M.G.**, **Riera, R.** and **Parker, J.H.** (2020) Widespread seagrass meadows during the Early Miocene (Burdigalian) in southwestern Australia paralleled modern seagrass distributions. *Palaeogeogr. Palaeoclimatol. Palaeoecol.*, **555**, 109846.

Hallenberger, M., **Reuning, L.**, **Gallagher, S.J.**, **Back, S.**, **Ishiwa, T.**, **Christensen, B.A.** and **Bogus, K.** (2019) Increased fluvial runoff terminated inorganic aragonite precipitation on the Northwest Shelf of Australia during the early Holocene. *Sci. Rep.*, **9**, 1–9.

Hallock, P. (1985) Why are Larger Foraminifera Large ? *Paleobiology*, **11**, 195–208.

Hallock, P. (1987) Fluctuation in the trophic resource continuum: a factor in global diversity cycles? *Paleoceanography*, **2**, 457–471.

Hallock, P. and **Glenn, E.C.** (1985) Numerical Analysis of Foraminiferal Assemblages : A Tool for Recognizing Depositional Facies in Lower Miocene Reef Complexes. *J. Paleontol.*, **59**, 1382–1394.

Hallock, P. and **Glenn, E.C.** (1986) Larger Foraminifera: A Tool for Paleoenvironmental Analysis of Cenozoic Carbonate Depositional Facies. *Palaios*, **1**, 55.

Hallock, P. and **Pomar, L.** (2008) Cenozoic evolution of larger benthic foraminifers : paleoceanographic evidence for changing habitats. In: *Proceeding of the 11th Session International Coral Reef Symposium* (Eds Riegl, B.M. and Dodge, R.E.), pp. 7–11. HCNSO at NSUWork, Ft. Lauderdale, FL.

Hatcher, B.G. (1991) Coral reefs in the Leeuwin Current - an ecological perspective. *J. R. Soc. West. Aust.*, **74**, 115–127.

Hillis, R.R., **Sandiford, M.**, **Reynolds, S.D.** and **Quigley, M.C.** (2008) Present-day stresses, seismicity and Neogene-to-Recent tectonics of Australia's 'passive' margins: intraplate deformation controlled by plate boundary forces. *Geol. Soc. London. Spec. Publ.*, **306**, 71–90.

Hocking, R.M., **Moors, H.T.** and **Graaff, W.J.** (1987) Geology of the Carnarvon Basin, Western Australia. In: *Bulletin 133*, pp. 307. Geological Survey of Western Australia, Perth, WA.

Hohenegger, J. (2006) The importance of symbiont-bearing benthic foraminifera for West Pacific carbonate beach environments. *Mar. Micropaleontol.*, **61**, 4–39.

Hottinger, L. (1997) Shallow benthic foraminiferal assemblages as signals for depth of their deposition and their limitations. *Bull. La Soc. Geol. Fr.*, **168**, 491–505.

Isern, A.R., **Anselmetti, F.S.** and **Blum, P.** (2005) A Neogene carbonate platform, slope, and shelf edifice shaped by sea level and ocean currents, Marion Plateau (northeast Australia). *AAPG Mem.*, 297–307.

Isern, A.R., **Mckenzie, J.A.** and **Feary, D.A.** (1996) The role of sea-surface temperature as a control on carbonate

platform development in the western Coral Sea. *Palaeogeogr. Palaeoclimatol. Palaeoecol.*, **124**, 247–272.

James, N.P. (1997) The cool-water carbonate depositional realm. *SEPM Spec. Public.*, **56**, 1–20.

James, N.P., Bone, Y., Kyser, T.K., Dix, G.R. and Collins, L.B. (2004) The importance of changing oceanography in controlling late Quaternary carbonate sedimentation on a high-energy, tropical, oceanic ramp: North-western Australia. *Sedimentology*, **51**, 1179–1205.

James, N.P. and von der Borch, C.C. (1991) Carbonate shelf edge off southern Australia: A prograding open-platform margin. *Geology*, **19**, 1005–1008.

James, N.P., Collins, L.B., Bone, Y. and Hallock, P. (1999) Subtropical carbonates in a temperate realm: modern sediments on the Southwest Australian Shelf. *J. Sediment. Res.*, **69**, 1297–1321.

John, C.M., Karner, G.D., Browning, E., Leckie, R.M., Mateo, Z., Carson, B. and Lowery, C. (2011) Timing and magnitude of Miocene eustasy derived from the mixed siliciclastic-carbonate stratigraphic record of the northeastern Australian margin. *Earth Planet. Sci. Lett.*, **304**, 455–467.

Jones, H.A. (1973) *Marine Geology of the Northwest Australian Continental Shelf*. Bulletin of the Bureau of Minerals Resources, Geology and Geophysics. Australian Government Publishing Service, Canberra, ACT, **136**, 58 pp.

Keep, M., Harrowfield, M. and Crowe, W. (2007) The Neogene tectonic history of the North West Shelf, Australia. *Explor. Geophys.*, **38**, 151–174.

Kiessling, W. (2001) Phanerozoic Reef Trends Based on the Paleoreef Database. In: *The History and Sedimentology 01 Ancient Reel Systems* (Ed. Stanley, G.D.J.), pp. 41–88. Kluwer Academic/Plenum Publishers, New York, NY.

Kominz, M.A., Browning, J.V., Miller, K.G., Sugarman, P.J., Mizintseva, S. and Scotese, C.R. (2008) Late Cretaceous to Miocene sea-level estimates from the New Jersey and Delaware coastal plain coreholes: an error analysis. *Basin Res.*, **20**, 211–226.

Krüger, R., Röttger, R., Lietz, R. and Hohenegger, J. (1997) Biology and Reproductive Processes of the Larger Foraminiferan Cycloclypeus carpenteri (Protozoa, Nummulitidae). *Arch. für Protistenkd.*, **147**, 307–321.

Kuhnt, W., Holbourn, A., Xu, J., Opdyke, B., De Deckker, P., Röhl, U. and Mudelsee, M. (2015) Southern Hemisphere control on Australian monsoon variability during the late deglaciation and Holocene. *Nat. Commun.*, **6**, 5916.

Langer, M.R. and Hottinger, L. (2000) Biogeography of Selected "Larger" Foraminifera. *Micropaleontology*, **46**, 105–126.

Liu, C., Fulthorpe, C.S., Austin, J.A. and Sanchez, C.M. (2011) Geomorphologic indicators of sea level and lowstand paleo-shelf exposure on early-middle Miocene sequence boundaries. *Mar. Geol.*, **280**, 182–194.

Logan, B.W. and Cebulski, D.E. (1970) Sedimentary Environments of Shark Bay, Western Australia. In: *Environments, Shark Bay, Western Australia, American Association of Petroleum Geologists Memoir 13* (Eds Logan, B.W., Davies, G.R., Read, J.F. and Cebulski, D.E.), pp. 1–37. AAPG, Tulsa, OK.

Lüdmann, T., Betzler, C., Eberli, G.P., Reolid, J., Reijmer, J.J.G., Sloss, C.R., Bialik, O.M., Alvarez-Zarikian, C.A., Alonso-García, M., Blättler, C.L., Guo, J.A., Haffen, S., Horozal, S., Inoue, M., Jovane, L., Kroon, D., Lanci, L., Laya, J.C., Mee, A.L.H., Nakakuni, M., Nath, B.N., Niino, K., Petruny, L.M., Pratiwi, S.D., Slagle, A.L., Su, X.,

Swart, P.K., Wright, J.D., Yao, Z. and Young, J.R. (2018) Carbonate delta drift: A new sediment drift type. *Mar. Geol.*, **401**, 98–111.

Lüdmann, T., Paulat, M., Betzler, C., Möbius, J., Lindhorst, S., Wunsch, M. and Eberli, G.P. (2016) Carbonate mounds in the Santaren Channel, Bahamas: A current-dominated periplatform depositional regime. *Mar. Geol.*, **376**, 69–85.

Lukasik, J.J., James, N.P., Gowran, B.M.C. and Bone, Y. (2000) An epeiric ramp: low-energy, cool-water carbonate facies in a Tertiary inland sea, Murray Basin, South Australia. *Sedimentology*, **47**, 851–881.

Malcolm, R.J., Pott, M.C. and Delfos, E. (1991) A new tectono-stratigraphic synthesis of the North West Cape Area. *APEA J.*, **31**, 154–174.

Mancosu, A. and Nebelsick, J.H. (2017) Palaeoecology and taphonomy of spatangoid-dominated echinoid assemblages: A case study from the Early-Middle Miocene of Sardinia, Italy. *Palaeogeogr. Palaeoclimatol. Palaeoecol.*, **466**, 334–352.

Martin, H.A. (2006) Cenozoic climatic change and the development of the arid vegetation in Australia. *J. Arid Environ.*, **66**, 533–563.

Mateu-Vicens, G., Hallock, P. and Brandano, M. (2008) A Depositional Model and Paleoecological Reconstruction of the Lower Tortonian Distally Steepened Ramp of Menorca (Balearic Islands, Spain). *Palaios*, **23**, 465–481.

Maurizot, P., Cabioch, G., Fournier, F., Leonide, P., Sebih, S., Rouillard, P., Montaggioni, L., Collot, J., Martin-Garin, B., Chaproniere, G., Braga, J.C. and Sevin, B. (2016) Post-obduction carbonate system development in New Caledonia (Népoui, Lower Miocene). *Sediment. Geol.*, **331**, 42–62.

McArthur, J.M. and Howarth, R.J. (2005) Strontium Isotope Stratigraphy. In: *A Geologic Time Scale 2004* (Eds Gradstein, F.M., Ogg, J.G. and Smith, A.G.), pp. 96–105. Cambridge University Press, Cambridge.

McCaffrey, J.C., Wallace, M.W. and Gallagher, S.J. (2020) A Cenozoic Great Barrier Reef on Australia's North West shelf. *Glob Planet Change*, **184**, 103048.

McGowran, B., Li, Q., Cann, J., Padley, D., McKirdy, D.M. and Shafik, S. (1997) Biogeographic impact of the Leeuwin Current in Southern Australia since the late middle Eocene. *Palaeogeogr. Palaeoclimatol. Palaeoecol.*, **136**, 19–40.

McNamara, K.J. and Kendrick, G.W. (1994) Cenozoic Molluscs and Echinoids of Barrow Island, Western Australia. *Rec. West. Aust. Museum*, **51**, 50.

Michel, J., Borgomano, J. and Reijmer, J.J.G. (2018) Heterozoan carbonates: When, where and why? A synthesis on parameters controlling carbonate production and occurrences. *Earth-Science Rev.*, **182**, 50–67.

Miller, K.G., Kominz, M.A., Browning, J.V., Wright, J.D., Mountain, G.S., Katz, M.E., Sugarman, P.J., Cramer, B.S., Christie-Blick, N. and Pekar, S.F. (2005) The Phanerozoic record of global sea-level change. *Science*, **310**, 1293–1298.

Moss, G.D., Cathro, D.L. and Austin, J.A. (2004) Sequence Biostratigraphy of Prograding Clinoforms, Northern Carnarvon Basin, Western Australia: A Proxy for Variations in Oligocene to Pliocene Global Sea Level? *Palaios*, **19**, 206–226.

Mudelsee, M., Bickert, T., Lear, C.H. and Lohmann, G. (2014) Cenozoic climate changes: A review based on time series analysis of marine benthic δ18O records. *Rev. Geophys.*, **52**, 333–374.

Müller, R.D., Cannon, J., Qin, X., Watson, R.J., Gurnis, M., Williams, S., Pfaffelmoser, T., Seton, M., Russell, S.H.J. and Zahirovic, S. (2018) GPlates: Building a virtual earth

through deep time. *Geochemistry. Geophys. Geosystems*, **19**, 2243–2261.

Novak, V. and Renema, W. (2018) Ecological tolerances of Miocene larger benthic foraminifera from Indonesia. *J. Asian Earth Sci.*, **151**, 301–323.

O'Connell, L.G., James, N.P. and Bone, Y. (2012) The Miocene Nullarbor Limestone, southern Australia; deposition on a vast subtropical epeiric platform. *Sediment. Geol.*, **253–254**, 1–16.

Parker, J.H. and Gischler, E. (2015) Modern and relict foraminiferal biofacies from a carbonate ramp, offshore Kuwait, northwest Persian Gulf. *Facies*, **61**(10), 1–22.

Pettijohn, F.J., Potter, P.E. and Siever, R. (1972) *Sand and Sandstone*. Springer-Verlag, Berlin, 618 pp.

Piller, W.E. and Mansour, A.M. (1994) Origin and Transport Mechanisms of Non-Carbonate Sediments in a Carbonate-Dominated Environment (Northern Safaga Bay, Red Sea, Egypt). *Abhandlunger der Geol. Bundesanstalt Wien*, **50**, 369–379.

Pomar, L. (2001a) Types of carbonate platforms: A genetic approach. *Basin Res.*, **13**, 313–334.

Pomar, L. (2001b) Ecological control of sedimentary accommodation: Evolution from a carbonate ramp to rimmed shelf, Upper Miocene, Balearic Islands. *Palaeogeogr. Palaeoclimatol. Palaeoecol.*, **175**, 249–272.

Pomar, L., Baceta, J.I., Hallock, P., Mateu-Vicens, G. and Basso, D. (2017) Reef building and carbonate production modes in the west-central Tethys during the Cenozoic. *Mar. Pet. Geol.*, **83**, 261–304.

Pomar, L. and Kendall, C.G.S.C. (2008) Architecture of Carbonate Platforms: A Response to Hydrodynamics and Evolving Ecology. *Soc. Econ. Paleontol. Mineral. Spec. Publ.*, **89**, 187–216.

Pomar, L., Morsilli, M., Hallock, P. and Bádenas, B. (2012) Internal waves, an under-explored source of turbulence events in the sedimentary record. *Earth-Science Rev.*, **111**, 56–81.

Power, M. (2008) Miocene carbonate reef complexes in the Browse Basin and the implication for drilling operations. *APPEA J.*, **48**, 115–132.

Purcell, P.G. and Purcell, R.R. (1988) The North West Shelf, Australia - an introduction. In: *The North West Shelf, Australia* (Eds Purcell, P.G. and Purcell, R.R.), *Proceedings of the Petroleum Exploration Society of Western Australia Symposium, Perth*, 3–15.

Rankey, E.C. (2017) Seismic architecture and seismic geomorphology of heterozoan carbonates: Eocene-Oligocene, Browse Basin, Northwest Shelf, Australia. *Mar. Pet. Geol.*, **82**, 424–443.

Reineck, H.-E. and Singh, I.B. (1980) *Depositional Sedimentary Environments*. Springer-Verlag, Berlin, 549 pp.

Renema, W. (2007) Fauna Development of Larger Benthic Foraminifera in the Cenozoic of Southeast Asia. In: *Biogeography, Time, and Place: Distributions, Barriers, and Islands. Topics In Geobiology*, vol 29 (Ed. Renema, W.), pp. 179–215. Springer, Dordrecht.

Renema, W. (2018) Terrestrial influence as a key driver of spatial variability in large benthic foraminiferal assemblage composition in the Central Indo-Pacific. *Earth-Sci. Rev.*, **177**, 514–544.

Renema, W. and Troelstra, S.R. (2001) Larger foraminifera distribution on a mesotrophic carbonate shelf in SW Sulawesi (Indonesia). *Palaeogeogr. Palaeoclimatol. Palaeoecol.*, **175**, 125–146.

Rex, R.W. and Goldberg, E.D. (1958) Quartz Contents of Pelagic Sediments of the Pacific Ocean. *Tellus*, **10**, 153–159.

Rexilius, J.P. and Powell, S.L. (1994a) Micropalaeontological analysis Pyrenees-1, Permit WA-155P, Carnarvon Basin, 23 pp.

Rexilius, J.P. and Powell, S.L. (1994b) Micropalaeontological analysis Macedon-1, Permit WA-155P, Carnarvon Basin, 25 pp.

Riera, R. (2020) Late Oligocene to Late Miocene evolution of carbonate platforms in the Exmouth-Barrow sub-basins (southern NWS, Australia). In: *Stratigraphic Evolution of Miocene Carbonate Platforms of the North West Shelf*. PhD Thesis, pp. 127–177. University of Western Australia, Perth, WA.

Riera, R., Bourget, J., Håkansson, E., Paumard, V. and Wilson, M.E.J. (2021) Middle Miocene tropical oligotrophic lagoon deposit sheds light on the origin of the Western Australian coral reef province. *Palaeogeogr. Palaeoclimatol. Palaeoecol.*, **576**, 110501.

Riera, R., Haig, D.W. and Bourget, J. (2019) Stratigraphic revision of the Miocene Trealla Limestone (Cape Range, Western Australia): Implications for Australasian foraminiferal biostratigraphy. *J. Foraminifer. Res.*, **49**, 318–338.

Rinke-Hardekopf, L., Reuning, L., Bourget, J. and Back, S. (2018) Syn-sedimentary deformation as a mechanism for the initiation of submarine gullies on a carbonate platform to slope transition, Browse Basin, Australian North West Shelf. *Mar. Pet. Geol.*, **91**, 622–630.

Romine, K.K., Durrant, J.M., Cathro, D.L. and Bernardel, G. (1997) Petroleum Play Element Prediction for the Cretaceous-Tertiary Basin Phase, Northern Carnarvon Basin. *APPEA J.*, **37**, 315–339.

Rosleff-Soerensen, B., Reuning, L., Back, S. and Kukla, P. (2012) Seismic geomorphology and growth architecture of a Miocene barrier reef, Browse Basin, NW-Australia. *Mar. Pet. Geol.*, **29**, 233–254.

Rosleff-Soerensen, B., Reuning, L., Back, S. and Kukla, P.A. (2016) The response of a basin-scale Miocene barrier reef system to long-term, strong subsidence on a passive continental margin, Barcoo Sub-basin, Australian North West Shelf. *Basin Res.*, **28**, 103–123.

Ryan, G.J., Bernardel, G., Kennard, J.M., Jones, A.T., Logan, G.A. and Rollet, N. (2009) A precursor extensive Miocene reef system to the Rowley Shoals reefs, WA: evidence for structural control of reef growth or natural hydrocarbon seepage. *APPEA J.*, **49**, 337–363.

Sandiford, M. (2007) The tilting continent: A new constraint on the dynamic topography field from Australia. *Earth Planet. Sci. Lett.*, **261**, 152–163.

Sangiorgi, F., Bijl, P.K., Passchier, S., Salzmann, U., Schouten, S., McKay, R., Cody, R.D., Pross, J., Van De Flierdt, T., Bohaty, S.M., Levy, R., Williams, T., Escutia, C. and Brinkhuis, H. (2018) Southern Ocean warming and Wilkes Land ice sheet retreat during the mid-Miocene. *Nat. Commun.*, **9**, 1–11.

Saqab, M.M. and Bourget, J. (2016) Seismic geomorphology and evolution of early–mid Miocene isolated carbonate build-ups in the Timor Sea, North West Shelf of Australia. *Mar. Geol.*, **379**, 224–245.

Saqab, M.M., Bourget, J., Trotter, J. and Keep, M. (2017) New constraints on the timing of flexural deformation along the northern Australian margin: Implications for arc-continent collision and the development of the Timor Trough. *Tectonophysics*, **696–697**, 14–36.

Seton, M., **Müller, R.D.**, **Zahirovic, S.**, **Gaina, C.**, **Torsvik, T.**, **Shephard, G.**, **Talsma, A.**, **Gurnis, M.**, **Turner, M.**, **Maus, S.** and **Chandler, M.** (2012) Global continental and ocean basin reconstructions since 200Ma. *Earth-Sci. Rev.*, **113**, 212–270.

Shevenell, A.E., **Kennett, J.P.** and **Lea, D.W.** (2004) Middle Miocene Southern Ocean Cooling and Antarctic Cryosphere Expansion. *Science*, **305**, 1766–1770.

Smith, R.L. (1992) Coastal upwelling in the modern ocean. *Geol. Soc. London. Spec. Publ.*, **64**, 9–28.

Stuut, J.-B.-W., **Temmesfeld, F.** and **De Deckker, P.** (2014) A 550 ka record of aeolian activity near North West Cape, Australia: inferences from grain-size distributions and bulk chemistry of SE Indian Ocean deep-sea sediments. *Quat. Sci. Rev.*, **83**, 83–94.

Teillet, T., **Fournier, F.**, **Montaggioni, L.F.**, **BouDagher-Fadel, M.**, **Borgomano, J.**, **Braga, J.C.**, **Villeneuve, Q.** and **Hong, F.** (2020) Development patterns of an isolated oligo-mesophotic carbonate buildup, early Miocene, Yadana field, offshore Myanmar. *Mar. Pet. Geol.*, **111**, 440–460.

Van Tuyl, J., **Alves, T.M.** and **Cherns, L.** (2018a) Geometric and depositional responses of carbonate build-ups to Miocene sea level and regional tectonics offshore northwest Australia. *Mar. Pet. Geol.*, **94**, 144–165.

Van Tuyl, J., **Alves, T.M.** and **Cherns, L.** (2018b) Pinnacle features at the base of isolated carbonate buildups marking point sources of fluid offshore Northwest Australia. *GSA Bull.*, **130**, 1596–1614.

Van Tuyl, J., **Alves, T.**, **Cherns, L.**, **Antonatos, G.**, **Burgess, P.** and **Masiero, I.** (2019) Geomorphological evidence of carbonate build-up demise on equatorial margins: A case study from offshore northwest Australia. *Mar. Pet. Geol.*, **104**, 125–149.

Veevers, J.J. and **Cotterill, D.** (1978) Western margin of Australia: Evolution of a rifted arch system. *Bull. Geol. Soc. Am.*, **89**, 337–355.

Wade, B.S., **Pearson, P.N.**, **Berggren, W.A.** and **Pälike, H.** (2011) Review and revision of Cenozoic tropical planktonic foraminiferal biostratigraphy and calibration to the geomagnetic polarity and astronomical time scale. *Earth-Science Rev.*, **104**, 111–142.

Wallace, M.W., **Condilis, E.**, **Powell, A.**, **Redfearn, J.**, **Auld, K.**, **Wiltshire, M.**, **Holdgate, G.** and **Gallagher, S.** (2003) Geological controls on sonic velocity in the Cenozoic carbonates of the Northern Carnarvon Basin, Northwest Shelf, Western Australia. *APPEA J.*, **43**, 385–399.

Webster, J.M., **Braga, J.C.**, **Humblet, M.**, **Potts, D.C.**, **Iryu, Y.**, **Yokoyama, Y.**, **Fujita, K.**, **Bourillot, R.**, **Esat, T.M.**, **Fallon, S.**, **Thompson, W.G.**, **Thomas, A.L.**, **Kan, H.**, **McGregor, H.V.**, **Hinestrosa, G.**, **Obrochta, S.P.** and **Lougheed, B.C.** (2018) Response of the Great Barrier Reef to sea-level and environmental changes over the past 30,000 years. *Nat. Geosci.*, **11**, 426–432.

Westphal, H. and **Aigner, T.** (1997) Seismic stratigraphy and subsidence analysis in the Barrow-Dampier Subbasin, Northwest Australia. *Am. Assoc. Pet. Geol. Bull.*, **81**, 1721–1749.

Westphal, H., **Halfar, J.** and **Freiwald, A.** (2010) Heterozoan carbonates in subtropical to tropical settings in the present and past. *Int. J. Earth Sci.*, **99**, 153–169.

Wilson, M.E.J. and **Lokier, S.W.** (2002) Siliciclastic and volcaniclastic influences on equatorial carbonates: Insights from the Neogene of Indonesia. *Sedimentology*, **49**, 583–601.

Wilson, M.E.J. and **Vecsei, A.** (2005) The apparent paradox of abundant foramol facies in low latitudes: Their environmental significance and effect on platform development. *Earth-Science Rev.*, **69**, 133–168.

Wyrwoll, K.H., **Greenstein, B.J.**, **Kendrick, G.W.** and **Chen, G.S.** (2009) The palaeoceanography of the Leeuwin Current: Implications for a future world. *J. R. Soc. West. Aust.*, **92**, 37–51.

Young, H.C. (2001) *The Sequence Stratigraphic Evolution of the Exmouth-Barrow Margin, Western Australia.* PhD Thesis. University of South Australia, Adelaide, SA, 298 pp.

Young, H.C., **Lemon, N.M.** and **Hull, J.N.F.** (2001) The Middle Cretaceous to Recent Sequence Stratigraphic Evolution of the Exmouth-Barrow Margin, Western Australia. *APPEA J.*, **41**, 381–413.

Zachos, J., **Pagani, M.**, **Sloan, L.**, **Thomas, E.** and **Billups, K.** (2001) Trends, Global Rhythms, Aberrations in Global Climate 65Ma to Present. *Science*, **292**, 686–693.